8e. Gamma Rays

ROBLEY D. EVANS

Massachusetts Institute of Technology

8e-1. Attenuation of Gamma Rays and X Rays. *The Photon.* Photons are classified according to their mode of origin, not their quantum energy. *Gamma rays* are the electromagnetic radiations which accompany nuclear transitions. *X rays* are the electromagnetic radiations which accompany electronic transitions, including the characteristic or fluorescent line spectra of X rays, the bremsstrahlung or continuous spectra of X rays, and the positron-negatron annihilation radiation. By extension, the X-ray category includes all photons originating outside an atomic nucleus and due to the transitions of other elementary particles, for example, proton bremsstrahlung, mu-mesonic X rays, and π^0-decay photons. In this section we deal only with the interaction of photons with matter. These interactions are thought to be independent of the origin of the photon. Hence we use the term photon to refer here to both γ rays and X rays.

The quantum energy of a photon is $E = h\nu$, where ν is the frequency and $h = 4.135 \times 10^{-21}$ MeV sec is Planck's constant. The corresponding wavelength is $\lambda = c/\nu = hc/E = 0.012\,397 \times 10^{-8}/E$ cm, when E is in MeV.

Competing Interactions. A photon can interact with matter by any one of several competing alternative mechanisms. For details, see refs. B3, E1, F3, G1, and G2. In each case the interaction is an all-or-nothing affair. The interaction can be with the entire atom (photoelectric effect and Rayleigh scattering) or with one electron in the atom (Compton effect and pair production in the field of an electron) or with the atomic nucleus (pair production, resonance elastic scattering, photodisintegration, and meson production). The probability for each of these many competing independent processes can be expressed as a collision cross section per atom, per electron, or per nucleus in the absorber. The sum of all these cross sections (corrected for coherence in some low-energy cases), normalized to a per atom basis, is then the probability that the incident photon will have an interaction of some kind while passing through a very thin absorber which contains one atom per cm^2 of area normal to the path of the incident photon.

Attenuation, Scattering, and Absorption. The total collision cross section per atom, when multipled by the number of atoms per cm^3 of absorber, is then the *linear attenuation coefficient* μ_0 per centimeter of travel in the absorber. The fraction of incident photons which can pass through a thickness x of absorber whose density is ρ without having an interaction of any kind is $e^{-\mu_0 x}$ or $e^{-(\mu_0/\rho)(\rho x)}$, where ρ is the density of the medium and μ_0/ρ is the mass attenuation coefficient.

The absorption coefficient μ_a is a much more restricted concept than the attenuation coefficient μ_0. Attenuation can be by some purely elastic process, such as Rayleigh scattering or nuclear resonance (Mössbauer) scattering, in which the photon is merely deflected and does not give up any of its initial energy to the medium. Here only a scattering coefficient would be involved. However, in a photoelectric interaction,

the entire energy of the incident photon is truly absorbed by an atom of the medium; there is no scattered residual photon. Here the attenuation of the primary radiation is due to complete absorption of the energy of the incident photon. The intermediate case of greatest importance is the Compton effect, in which some energy is absorbed and appears in the medium as kinetic energy of a Compton recoil electron while the balance of the incident energy is not absorbed but is present as a Compton scattered photon. *Scattering*, then, involves the deflection of incident photon energy, *absorption* involves the conversion of incident photon energy into the kinetic energy of a

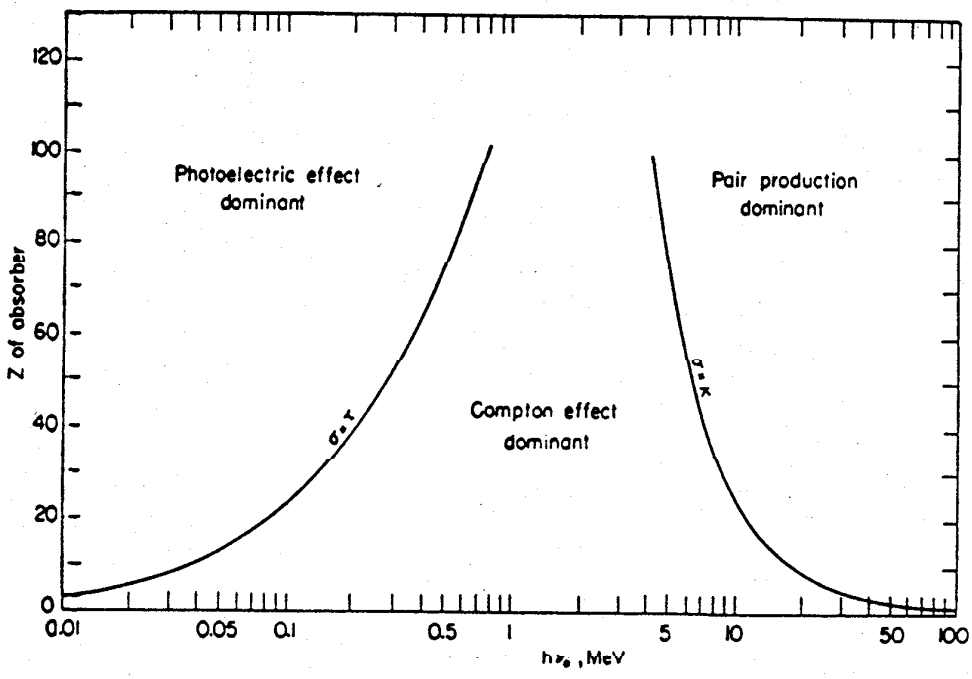

FIG. 8e-1. Relative importance of the three major types of γ-ray interaction. The lines show the values of Z and $h\nu$ for which the two neighboring effects are just equal. [*From Evans* (E1).]

charged particle (usually an electron; see Sec. 8e-5), and the *attenuation* coefficient μ_0 is the sum of the scattering coefficient μ_s and the absorption coefficient μ_a, or

$$\mu_0 = \mu_s + \mu_a \tag{8e-1}$$

In most practical cases μ_s is simply the Compton scattering coefficient σ_s of Eqs. (8e-25) and (8e-34) (see page 720 of ref. E1).

Compton, Photoelectric, and Pair-production Competition. In the energy domain met most frequently, say 0.01 to 10 MeV, all but a few minor effects are due to only three of the many competing processes. These are the Compton effect, the photoelectric effect, and pair production. Figure 8e-1 provides a handy guide to the relative importance of these three principal interactions over broad ranges of energies $h\nu_0$ of the incident photons and atomic numbers Z of the attenuating material. For any Z the Compton effect predominates for photon energies between 0.8 and 4 MeV; for low-Z materials the Compton effect predominates over a much wider domain of photon energies. For moderately large Z, the photoelectric interaction is dominant at very small $h\nu_0$ and the pair-production interaction is dominant at large $h\nu_0$.

Nuclear Disintegrations by High-energy Photons. The "separation energy," or energy required to remove one neutron or one proton from a nucleus, differs from the average binding energy per nucleon and, for most stable middleweight or heavyweight nuclei, lies in the domain of about 6 to 16 MeV (see ref. E4 for a brief discussion). Above these appropriate individual threshold energies a nucleus can absorb a photon and emit a neutron in a (γ,n) reaction, or emit a proton in a (γ,p) reaction. Above the threshold energy, the cross section for these *photonuclear reactions* increases with increasing photon energy $h\nu$, reaches a maximum value, then decreases with further increases of $h\nu$. The shape of this peak is characteristic of resonance reactions and is called *the giant resonance.* Typically, the maximum value of this photonuclear cross section in most light elements is reached at about 20 to 25 MeV, and in heavy elements at smaller photon energies down to about 13 MeV in uranium. The peak value of the giant resonance in the (γ,n) cross section is typically of the order of 10 millibarns in light elements, and increases with mass number to the order of a few hundred millibarns in heavy elements. The (γ,p) cross section is generally smaller than the (γ,n) cross section because of the nuclear Coulomb barrier against proton emission.

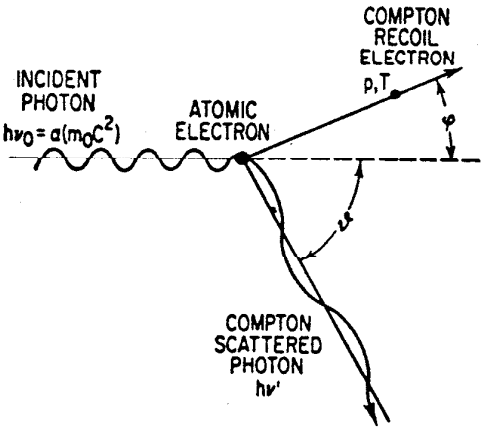

FIG. 8e-2. Trajectories in the scattering plane for the incident photon $h\nu_0$, the scattered photon $h\nu'$, and the scattering electron which acquires momentum p and kinetic energy T.

In all cases, the maximum value of the total cross section for all photonuclear reactions is smaller than about 5 percent of the total cross section for Compton and pair-production interactions. Thus in nearly all practical cases the energy absorbed from a high-energy photon beam by any medium is not materially increased by photonuclear interactions.

In very heavy nuclei, photon absorption can also induce fission. The threshold for *photofission* in various isotopes of Th, U, and Pu is between 5.0 and 5.5 MeV. The photofission cross section for U^{238} has a giant resonance shape, a peak cross section of 125 millibarns at 14 MeV, and a full width at half maximum of 8.8 MeV. Again the cross section is very small compared with the cross section for pair production (19 barns) and Compton interactions (3 barns) in uranium at 14 MeV.

When nuclei absorb photons whose energy is above about 140 MeV, pi mesons can be produced in reactions such as $p(\gamma,\pi^+)n$. The cross section for *meson production* rises slowly with photon energy above about 140 MeV, reaching values of about 0.2 millibarn at 250 MeV for $H(\gamma,\pi^+)n$. For other elements, the cross section varies approximately as $Z^{\frac{1}{3}}$. For comparison, the pair-production cross section at 250 MeV is about $6Z^2$ barns for all elements, or more than 10,000 times larger than the meson production cross section.

8e-2. Compton Effect. The incident photon has an energy $h\nu_0$ and momentum $p = h\nu_0/c$. It spends these on a single individual atomic electron in a given collision. If the initial binding energy of the electron is small compared with $h\nu_0$, then the struck electron can be considered initially free and unbound. Conservation of momentum and energy leads to the usual Compton equations, and the cross sections are given by the Dirac electron theory as first applied to the Compton collision by Klein and Nishina. As in Fig. 8e-2, the electron recoils at an angle φ with kinetic

energy T, and the remaining energy, $h\nu' = h\nu_0 - T$, is found in a Compton scattered photon emitted at an angle ϑ.

The *Compton shift* is the difference between the wavelength λ_0 (or the energy $h\nu_0$) of the incident photon and the wavelength λ' (or energy $h\nu'$) of the Compton scattered photon and is

$$\frac{1}{h\nu'} - \frac{1}{h\nu_0} = \frac{1}{m_0c^2}(1 - \cos\vartheta) \tag{8e-2}$$

or

$$\lambda' - \lambda_0 = \frac{h}{m_0c}(1 - \cos\vartheta) \tag{8e-3}$$

Note that the Compton shift in wavelength $(\lambda' - \lambda_0)$ in any particular direction is independent of the energy of the incident photon but that the Compton shift in energy $(h\nu_0 - h\nu')$ increases very strongly as $h\nu_0$ increases. The length $h/m_0c = \lambda_c = 2.426 \times 10^{-10}$ cm is called the Compton wavelength for an electron. It is equal to the wavelength of a photon whose energy is just equal to the rest energy of the electron $m_0c^2 = 0.5110$ MeV.

Writing the incident energy in terms of the dimensionless quantity

$$\alpha \equiv \frac{h\nu_0}{m_0c^2} \tag{8e-4}$$

the conservation laws give, for the energy of the Compton scattered photon,

$$\frac{\nu'}{\nu_0} = \frac{1}{1 + \alpha(1 - \cos\vartheta)} \tag{8e-5}$$

$$(h\nu')_{\min} = m_0c^2\frac{\alpha}{1 + 2\alpha} = h\nu_0\frac{1}{1 + 2\alpha} \qquad \text{for } \vartheta = 180 \text{ deg} \tag{8e-6}$$

Figure 8e-3 gives $h\nu'$ vs. $h\nu_0$ for 10 values of ϑ. The curve for $\vartheta = 180$ deg gives $(h\nu')_{\min}$ and thus evaluates the backscatter peak and the energy separation between the Compton edge and the total energy peak in γ-ray scintillation spectroscopy (see Sec. 8e-6). The energy of the backscattered photon $(h\nu'_{\min})$ approaches its maximum value of $m_0c^2/2 = 0.25$ MeV for high-energy incident photons, $\alpha \gg 1$.

The angle φ and the kinetic energy T of the Compton recoil electron are related to the photon scattering angle ϑ by

$$\cot\varphi = (1 + \alpha)\tan\frac{\vartheta}{2} \tag{8e-7}$$

$$T = h\nu_0 - h\nu' = h\nu_0\frac{\alpha(1 - \cos\vartheta)}{1 + \alpha(1 - \cos\vartheta)} \tag{8e-8}$$

$$T_{\max} = h\nu_0 - (h\nu')_{\min} = h\nu_0\frac{2\alpha}{1 + 2\alpha} \qquad \text{for } \vartheta = 180 \text{ deg} \tag{8e-9}$$

Klein-Nishina Collision Differential Cross Section. The *collision* differential cross section $d(_e\sigma)$, where the subscript connotes per electron in the attenuator, refers to the *number* of collisions of a particular type. The *number* of photons which are scattered in a particular direction, as a fraction of the *number* of incident photons, is $d(_e\sigma)$ and has the dimensions

$$d(_e\sigma) = \frac{\text{number scattered [number/(sec} \cdot \text{electron)]}}{\text{number incident [number/(cm}^2 \cdot \text{sec)]}} = \frac{\text{cm}^2}{\text{electron}} \tag{8e-10}$$

As first shown by Klein and Nishina, the collision differential cross section for unpolarized photons striking unbound, randomly oriented electrons is

$$d(_e\sigma) = \frac{r_0^2}{2}\,d\Omega\left(\frac{\nu'}{\nu_0}\right)^2\left(\frac{\nu_0}{\nu'} + \frac{\nu'}{\nu_0} - \sin^2\vartheta\right) \qquad \frac{\text{cm}^2}{\text{electron}} \tag{8e-11}$$

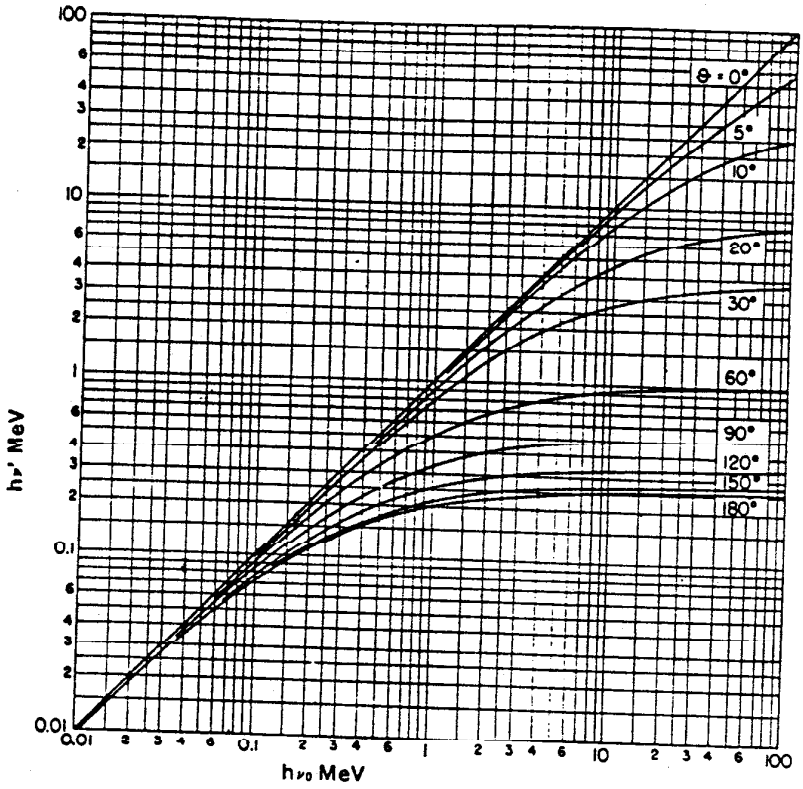

FIG. 8e-3. Dependence of the energy $h\nu'$ of the Compton-scattered photon on $h\nu_0$ and the photon scattering angle ϑ, from Eq. (8e-5). [*From Evans* (E2).]

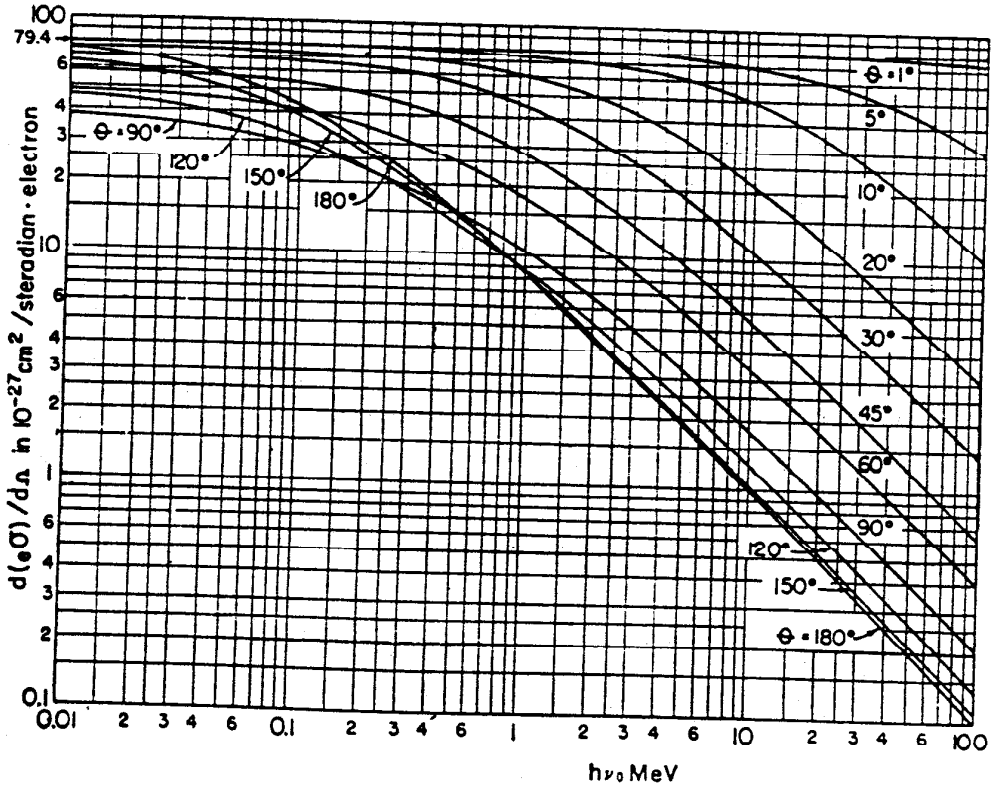

FIG. 8e-4. Collision differential cross section $d(e\sigma)/d\Omega$ for the *number* of photons scattered per unit solid angle in the direction ϑ. [*From Evans* (E2).]

where the scattered photon $h\nu'$ goes into the solid angle $d\Omega$ steradians at mean angle ϑ and the classical radius of the electron r_0 has the value

$$r_0 \equiv \frac{e^2}{m_0c^2} = 2.818 \times 10^{-13} \text{ cm} \tag{8e-12}$$

Substituting ν'/ν_0 in terms of ϑ and the incident photon energy $h\nu_0 = \alpha(m_0c^2)$ gives the equivalent explicit relationship

$$d(_e\sigma) = r_0^2\, d\Omega \left[\frac{1}{1 + \alpha(1 - \cos\vartheta)}\right]^2 \left(\frac{1 + \cos^2\vartheta}{2}\right) \left\{1 + \frac{\alpha^2(1 - \cos\vartheta)^2}{(1 + \cos^2\vartheta)[1 + \alpha(1 - \cos\vartheta)]}\right\} \quad \frac{\text{cm}^2}{\text{electron}} \tag{8e-13}$$

Table 8e-1 and Fig. 8e-4 give numerical values of $d(_e\sigma)/d\Omega$ in 10^{-27} cm^2 (or millibarn)/steradian per electron. The classical or Thomson differential cross section is

$$\frac{d(_e\sigma_{\text{Thom}})}{d\Omega} = r_0^2 \left(\frac{1 + \cos^2\vartheta}{2}\right) \quad \frac{\text{cm}^2}{\text{steradian} \cdot \text{electron}} \tag{8e-14}$$

TABLE 8e-1. COLLISION DIFFERENTIAL CROSS SECTION $d(_e\sigma)/d\Omega$ IN 10^{-27} CM^2/STERADIAN PER ELECTRON*
[From Eq. (8e-13)]

$h\nu_0$, MeV	ϑ										
	1°	5°	10°	20°	30°	45°	60°	90°	120°	150°	180°
0.01	79.4	79.1	78.1	74.6	69.1	59.0	48.6	38.3	46.4	64.7	73.6
0.04	79.4	79.0	78.0	74.0	68.0	57.5	45.5	34.4	40.4	53.5	60.2
0.1	79.4	79.0	77.7	73.0	66.0	53.7	41.0	29.3	31.3	39.2	43.2
0.2	79.4	78.8	77.3	71.3	62.8	48.2	35.0	22.9	23.0	27.2	29.3
0.4	79.4	78.6	76.4	68.2	57.2	41.0	28.5	16.8	15.7	17.2	17.9
1	79.3	77.9	73.7	60.2	45.0	27.7	17.7	10.4	8.80	8.45	8.35
2	79.3	76.8	69.7	50.1	33.0	18.3	11.5	6.80	5.30	4.73	4.54
4	79.2	74.6	62.8	37.3	21.7	11.5	7.15	4.09	2.98	2.50	2.39
10	78.9	68.6	48.4	21.2	11.0	5.6	3.48	1.86	1.28	1.05	0.98
20	78.4	60.4	34.2	12.5	6.3	2.93	1.86	0.97	0.66	0.535	0.498
40	77.6	48.6	22.0	7.00	3.40	1.56	0.97	0.492	0.336	0.270	0.254
100	75.0	30.5	10.5	3.08	1.45	0.64	0.40	0.204	0.135	0.108	0.102

* From R. D. Evans, Compton Effect, in "Handbuch der Physik," vol. XXXIV, pp. 218-298, S. Flügge, ed., Springer-Verlag, Berlin, 1958.

where $r_0^2 = 79.41 \times 10^{-27}$ cm^2 is the upper limit approached by this Klein-Nishina collision differential cross section at any ϑ as $\alpha = h\nu_0/m_0c^2$ approaches zero and at any α as ϑ approaches zero.

Klein-Nishina Scattering Differential Cross Section. The *scattering* differential cross section $d(_e\sigma_s)$ refers to the amount of *energy* scattered in a particular direction; thus

$$d(_e\sigma_s) = \frac{\text{scattered energy per sec [MeV/(sec} \cdot \text{electron)]}}{\text{incident intensity [MeV/(cm}^2 \cdot \text{sec)]}} = \frac{\text{cm}^2}{\text{electron}} \tag{8e-15}$$

The scattered *energy* is the number of scattered photons times the quantum energy $h\nu'$ of each, and the incident intensity is the number of incident photons per unit

area times the quantum energy $h\nu_0$ of each. Not all the energy $h\nu_0$ is scattered, but only the fraction $h\nu'/h\nu_0$. Therefore the *scattering* differential cross section for unpolarized radiation is

$$d(_e\sigma_s) = \frac{\nu'}{\nu_0}\, d(_e\sigma)$$
$$= \frac{r_0^2}{2}\, d\Omega \left(\frac{\nu'}{\nu_0}\right)^3 \left(\frac{\nu_0}{\nu'} + \frac{\nu'}{\nu_0} - \sin^2\vartheta\right) \qquad \frac{\text{cm}^2}{\text{electron}} \tag{8e-16}$$

Tables and graphs of $d(_e\sigma_s)$ over the range 1 deg $\leq \vartheta \leq$ 180 deg and 0.01 MeV $\leq h\nu_0 \leq$ 100 MeV are available in ref. E2.

Angular Distribution of the Number of Scattered Photons. The total solid angle available per unit scattering angle is

$$\frac{d\Omega}{d\vartheta} = 2\pi \sin\vartheta \tag{8e-17}$$

and approaches zero in the forward- and backward-scattering directions. The *number-vs.-angle* distribution of scattered photons is

$$\frac{d(_e\sigma)}{d\vartheta} = \frac{d(_e\sigma)}{d\Omega}\, 2\pi \sin\vartheta \qquad \frac{\text{cm}^2}{\text{electron} \cdot \text{radian}} \tag{8e-18}$$

and has a forward maximum which is in the vicinity of $\vartheta = 20$ deg for $h\nu_0 = 3$ MeV and is at larger angles for smaller $h\nu_0$ (see Fig. 20 of ref. E2).

Angular Distribution of the Energy of Scattered Photons. The distribution of scattered photon *energy* in any angular interval, that is, between two cones of half angles ϑ and $\vartheta + d\vartheta$, is

$$\frac{d(_e\sigma_s)}{d\vartheta} = \frac{d(_e\sigma_s)}{d\Omega}\, 2\pi \sin\vartheta \qquad \frac{\text{cm}^2}{\text{electron} \cdot \text{radian}} \tag{8e-19}$$

and is more sharply peaked than the number-vs.-angle distribution because of the variation of $h\nu'$ with ϑ (see fig. 24 of ref. E2).

Angular Distribution of Compton Recoil Electrons. The ionization which actuates many radiation detectors is due primarily to Compton recoil electrons produced in the detector or its walls and projected between $\varphi = 0$ and $\varphi = 90$ deg. The initial *number-vs.-angle* distribution of the recoil electrons is

$$\frac{d(_e\sigma)}{d\varphi} = \frac{d(_e\sigma)}{d\Omega}\left[\frac{2\pi(1 + \cos\vartheta)\sin\vartheta}{(1 + \alpha)\sin^2\varphi}\right] \qquad \frac{\text{cm}^2}{\text{electron} \cdot \text{radian}} \tag{8e-20}$$

For photon energies below about 0.5 MeV this distribution has two maxima, in the neighborhood of 20 and 60 deg. At higher photon energies the wide-angle maximum disappears and the small-angle maximum occurs at smaller angles as $h\nu_0$ increases (see fig. 21 of ref. E2 and table III of ref. J1).

Energy Distribution of Compton Recoil Electrons. The *number-vs.-energy* spectrum of Compton electrons is

$$\frac{d(_e\sigma)}{dT} = \frac{d(_e\sigma)}{d\Omega}\frac{d\Omega}{d\vartheta}\frac{d\vartheta}{dT}$$
$$= \frac{d(_e\sigma)}{d\Omega}\frac{2\pi m_0c^2}{(h\nu')^2} = \frac{d(_e\sigma)}{d\Omega}\frac{2\pi m_0c^2}{(h\nu_0 - T)^2}$$
$$= \frac{\pi r_0^2}{\alpha^2 m_0c^2}\left\{2 + \left(\frac{T}{h\nu_0 - T}\right)^2\left[\frac{1}{\alpha^2} + \frac{h\nu_0 - T}{h\nu_0} - \frac{2}{\alpha}\frac{(h\nu_0 - T)}{T}\right]\right\}$$
$$\frac{\text{cm}^2}{\text{keV} \cdot \text{electron}} \tag{8e-21}$$

where $r_0 = 2.818 \times 10^{-13}$ cm and $m_0c^2 = 511.0$ keV. The electron spectra for $h\nu_0 =$ 0.5 to 3.5 MeV, in steps of 0.5 MeV, are shown in Fig. 8e-5 (see also table II of ref. J1 and fig. VII of ref. N1). The pronounced number maximum which occurs just at the maximum electron energy T_{max} is called the *Compton edge* in γ-ray spectroscopy (see Sec. 8e-6).

Energy Distribution of Compton Scattered Photons. Each recoil electron has a companion scattered photon whose energy is $h\nu' = h\nu_0 - T$. Hence the energy spectrum

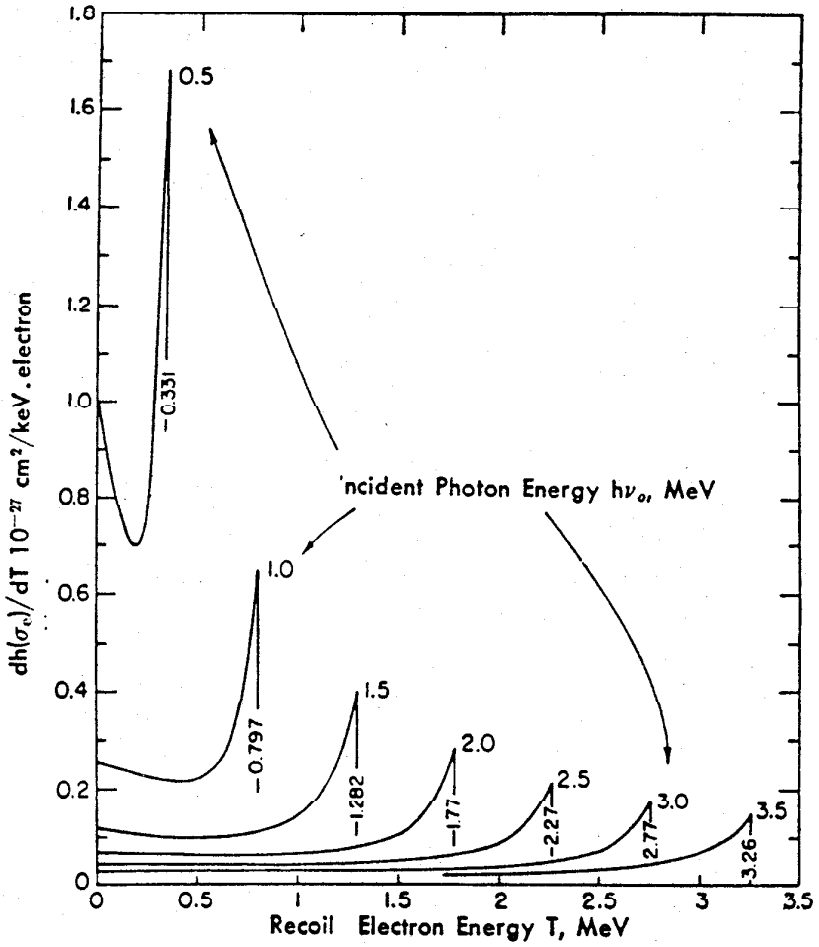

FIG. 8e-5. Number-vs.-energy distribution of Compton recoil electrons, for seven values of the incident photon energy $h\nu_0$, in 10^{-27} cm² (millibarn)/keV per free electron. The energy spectrum of scattered photons is obtained by transforming the energy scale from T to $h\nu_0 - T$ for each curve. [*From Evans* (E2).]

of scattered photons is complementary to the energy spectrum of recoil electrons and is given by replacing T by $(h\nu_0 - h\nu')$ and dT by $d(h\nu')$ in Eq. 8e-21 and in Fig. 8e-5.

Average Collision Cross Section. The average (or total) collision cross section $_e\sigma$ is the probability of any Compton interaction by one photon while passing normally through a material containing one electron per cm² and is given by

$$_e\sigma = \int_0^\pi \frac{d(_e\sigma)}{d\Omega}\, 2\pi \sin\vartheta\, d\vartheta = 2\pi r_0^2 \left\{ \frac{1+\alpha}{\alpha^2}\left[\frac{2(1+\alpha)}{1+2\alpha} - \frac{\ln(1+2\alpha)}{\alpha}\right] + \frac{\ln(1+2\alpha)}{2\alpha} - \frac{1+3\alpha}{(1+2\alpha)^2}\right\} \quad \frac{\text{cm}^2}{\text{electron}} \qquad (8e\text{-}22)$$

Numerical values are given in Table 8e-2 (see also fig. 27 of ref. E2 and fig. VIII of ref. N1). For small values of $\alpha \equiv h\nu_0/m_0c^2$, accuracy is best preserved by using the expansion

$$_e\sigma \simeq \frac{8}{3}\pi r_0^2\left(1 - 2\alpha + \frac{26}{5}\alpha^2 - \frac{133}{10}\alpha^3 + \frac{1{,}144}{35}\alpha^4 - \frac{544}{7}\alpha^5 + \frac{3{,}784}{20}\alpha^6 - \cdots\right) \quad \frac{\text{cm}^2}{\text{electron}} \tag{8e-23}$$

while for $\alpha \gg 1$,

$$_e\sigma \simeq \pi r_0^2 \frac{1 + 2\ln 2\alpha}{2\alpha} \quad \frac{\text{cm}^2}{\text{electron}} \tag{8e-24}$$

is a good approximation.

Average Scattering Cross Section. The total *scattered energy* in photons of various energies $h\nu'$, scattered on the average by each electron per cm² of scattering material, is the *average scattering cross section* $_e\sigma_s$ multiplied by the incident energy expressed as (number of photons) × (energy $h\nu_0$ per photon), where

$$\begin{aligned} _e\sigma_s &= \int_0^\pi \frac{d(_e\sigma_s)}{d\Omega} 2\pi \sin\vartheta\, d\vartheta \\ &= \pi r_0^2\left[\frac{\ln(1+2\alpha)}{\alpha^3} + \frac{2(1+\alpha)(2\alpha^2 - 2\alpha - 1)}{\alpha^2(1+2\alpha)^2} + \frac{8\alpha^2}{3(1+2\alpha)^3}\right] \quad \frac{\text{cm}^2}{\text{electron}} \end{aligned} \tag{8e-25}$$

For small α, use the expansion

$$_e\sigma_s = \frac{8}{3}\pi r_0^2\left(1 - 3\alpha + \frac{94}{10}\alpha^2 - 28\alpha^3 + \frac{552}{7}\alpha^4 - 212\alpha^5 + \frac{1{,}648}{3}\alpha^6 - \cdots\right) \quad \frac{\text{cm}^2}{\text{electron}} \tag{8e-26}$$

Table 8e-2 gives numerical values of $_e\sigma_s$ as well as the average energy $(h\nu')_{av}$ per scattered photon, which is

$$(h\nu')_{av} = h\nu_0 \frac{_e\sigma_s}{_e\sigma} \tag{8e-27}$$

Average Absorption Cross Section. The total *kinetic energy*, in recoil electrons of various kinetic energies T, produced on the average per electron per cm² of material is the *average absorption cross section* $_e\sigma_a$ multiplied by the incident energy expressed as (number of photons) × (energy $h\nu_0$ per photon), where

$$\begin{aligned} _e\sigma_a = {}_e\sigma - {}_e\sigma_s - 2\pi r_0^2\Bigg[&\frac{2(1+\alpha)^2}{\alpha^2(1+2\alpha)} - \frac{1+3\alpha}{(1+2\alpha)^2} - \frac{(1+\alpha)(2\alpha^2 - 2\alpha - 1)}{\alpha^2(1+2\alpha)^2} \\ &- \frac{4\alpha^2}{3(1+2\alpha)^3} - \left(\frac{1+\alpha}{\alpha^3} - \frac{1}{2\alpha} + \frac{1}{2\alpha^2}\right)\ln(1+2\alpha)\Bigg] \quad \frac{\text{cm}^2}{\text{electron}} \end{aligned} \tag{8e-28}$$

For small α, use the expansion

$$_e\sigma_a = \frac{8}{3}\pi r_0^2\left(\alpha - \frac{42}{10}\alpha^2 + \frac{147}{10}\alpha^3 - \frac{1{,}616}{35}\alpha^4 + \frac{940}{7}\alpha^5 - \frac{7{,}752}{21}\alpha^6 + \cdots\right) \quad \frac{\text{cm}^2}{\text{electron}} \tag{8e-29}$$

Table 8e-2 gives numerical values of $_e\sigma_a$ as well as the average energy T_{av} of the Compton recoil electrons, which is

$$T_{av} = h\nu_0 - (h\nu')_{av} = h\nu_0 \frac{_e\sigma_a}{_e\sigma} \tag{8e-30}$$

TABLE 8e-2. KLEIN-NISHINA CROSS SECTIONS FOR COMPTON INTERACTIONS IN 10^{-27} CM^2 (MILLIBARNS) PER FREE ELECTRON AND RELATED QUANTITIES*

[Calculated from the following equations: $_e\sigma$ (8e-22) and (8e-23), $_e\sigma_s$ (8e-25) and (8e-26), $_e\sigma_a$ (8e-28) and (8e-29), $(h\nu')_{av}$ (8e-27), T_{av} (8e-30), $T_{av}/h\nu_0$ (8e-30). Using $r_0 = 2.818 \times 10^{-13}$ cm and $m_0c^2 = 0.5110$ MeV]

Photon energy $h\nu_0$, MeV	Cross sections, 10^{-27} cm^2/electron			Scattered photon average energy $(h\nu')_{av}$, MeV	Recoil electron	
	Collision $_e\sigma$†	Scattering $_e\sigma_s$†	Absorption $_e\sigma_a$		Average energy $(T)_{av}$, MeV	Fraction of incident photon energy $(T)_{av}/h\nu_0$
0.010	640.5	628.5	12.0	0.0098	0.0002	0.0187
0.015	629.0	611.6	17.4	0.0146	0.0004	0.0277
0.020	618.0	595.7	22.3	0.0193	0.0007	0.0361
0.030	597.6	566.5	31.1	0.0284	0.0016	0.0520
0.040	578.7	540.1	38.6	0.0373	0.0027	0.0667
0.050	561.5	516.2	45.3	0.0460	0.0040	0.0807
0.060	545.7	494.5	51.2	0.0544	0.0056	0.0938
0.080	517.3	456.7	60.6	0.0706	0.0094	0.1171
0.100	492.8	424.8	68.0	0.0862	0.0138	0.1380
0.150	443.6	363.1	80.5	0.1228	0.0272	0.1815
0.200	406.5	318.6	87.9	0.1568	0.0432	0.2162
0.300	353.5	258.2	95.3	0.2191	0.0809	0.2696
0.400	316.7	218.6	98.1	0.276	0.124	0.3098
0.500	289.7	190.5	99.2	0.329	0.171	0.3424
0.600	267.5	169.2	98.3	0.379	0.221	0.3675
0.800	235.0	138.9	96.1	0.473	0.327	0.4089
1.00	211.2	118.3	92.9	0.560	0.440	0.4399
1.50	171.6	86.70	84.9	0.758	0.742	0.4948
2.00	146.4	68.67	77.7	0.939	1.061	0.5307
3.00	115.1	48.65	66.4	1.269	1.731	0.5769
4.00	95.98	37.73	58.25	1.57	2.428	0.6069
5.00	82.87	30.83	52.04	1.86	3.140	0.6280
6.00	73.23	26.07	47.16	2.14	3.864	0.6440
8.00	59.89	19.93	39.96	2.66	5.338	0.6672
10	50.99	16.14	34.85	3.16	6.835	0.6835
15	37.71	10.94	26.77	4.35	10.65	0.7099
20	30.25	8.272	21.98	5.47	14.53	0.7266
30	22.00	5.563	16.44	7.58	22.42	0.7473
40	17.46	4.191	13.27	9.6	30.4	0.7600
50	14.58	3.362	11.22	11.5	38.5	0.7695
60	12.54	2.807	9.733	13.4	46.6	0.7762
80	9.882	2.110	7.772	17.1	62.9	0.7865
100	8.199	1.690	6.509	20.6	79.4	0.7939

* From R. D. Evans, Compton Effect, in "Handbuch der Physik," vol. XXXIV, pp. 218-298, S. Flügge, ed., Springer-Verlag, Berlin, 1958.

† These numerical calculations for $_e\sigma$ and $_e\sigma_s$ were done on the IBM computer at the Massachusetts Institute of Technology under the direction of Mr. W. B. Thurston.

The fraction of the incident photon energy which is absorbed and appears as kinetic energy of Compton recoil electrons in the average of all Compton collisions is $T_{av}/h\nu_0 = {}_e\sigma_a/{}_e\sigma$. This fraction starts at zero for very low energy photons and increases monotonically with $h\nu_0$, as shown in the right-hand column of Table 8e-2.

The Compton collision (or attenuation) cross section is then the sum of the Compton scattering and absorption cross sections; that is,

$$\begin{aligned} {}_e\sigma &= \frac{(h\nu')_{av}}{h\nu_0}({}_e\sigma) + \frac{T_{av}}{h\nu_0}({}_e\sigma) \\ &= \frac{{}_e\sigma_s}{{}_e\sigma}({}_e\sigma) + \frac{{}_e\sigma_a}{{}_e\sigma}({}_e\sigma) \\ &= {}_e\sigma_s + {}_e\sigma_a \end{aligned} \tag{8e-31}$$

8e-3. Photoelectric Effect. The entire primary photon energy $h\nu$ is absorbed by the struck atom. One electron (usually from the K or L shell) is ejected with kinetic energy T, where

$$T = h\nu - B_e \tag{8e-32}$$

and B_e is binding energy of the electron before being ejected from the atom. Momentum is conserved by the backward recoil of the entire residual atom. The energy B_e is emitted promptly by the residual atom as characteristic X rays and Auger electrons from the filling of the vacancy in the inner shell. Because the entire atom participates in the interaction, photoelectric interactions are described by an *atomic* cross section ${}_a\tau$ cm²/atom. No single closed formula describes ${}_a\tau$ accurately over a wide range of $h\nu$. A crude but useful guide is

$${}_a\tau \simeq \text{const}\,\frac{Z^4}{(h\nu)^3} \tag{8e-33}$$

The experimental and theoretical material has been summarized in refs. D1, D2, E1, G2, and H3. Numerical tables of blended theoretical and experimental "best" values of ${}_a\tau$ for 11 elements from 0.01 to 100 MeV are given in ref. H3. Mainly owing to differences in the interpretation of experimental results, H3 values of ${}_a\tau$ at small $h\nu_0$ (<0.1 MeV) and large Z are smaller than D2 and larger than G2 values. For large $h\nu_0$ (>1 MeV) and large Z, ${}_a\tau$ is smaller in H3 and D2 than in G2, owing to revisions in the theoretical values. For 1 MeV and large Z there is agreement among D2, G2, and H3. Photoelectric mass absorption coefficients for air, water, Al, Cu, NaI, and Pb and interpolation formulas are given in Sec. 8e-5.

8e-4. Pair Production by Photons. In the field of a charged particle, usually an atomic nucleus but also to some degree in the field of an atomic electron, a photon may be totally absorbed and a positron-negatron pair emitted. A minimum incident photon energy of $h\nu = 2m_0c^2 = 1.02$ MeV is required for pair production in the field of a nucleus, and a minimum of $h\nu = 4m_0c^2 = 2.04$ MeV in the field of an atomic electron.

The atomic cross section ${}_a\kappa$ for nuclear pair production increases with Z^2 (reduced somewhat at very large photon energies by electron screening of the nuclear field) and with the photon energy $h\nu$. The kinetic energies of the positron and the negatron pair electrons are continuously distributed, each from a minimum of zero up to a maximum of $h\nu - 2m_0c^2$. Tables are given for 11 elements in ref. H3, and for 24 elements and several mixtures in ref. G2.

Analytical expressions for ${}_a\kappa$ are complicated (see ref. H1). Tables are given for 11 elements in ref. H3, and for 24 elements and several mixtures in ref. G2. Graphs and interpolation formulas are given in ref. E1 and in Sec. 8e-5.

8e-5. Mass Attenuation and Absorption Coefficients for Photons in Narrow-beam Geometry. Linear attenuation coefficients, σ (Compton), τ (photo), and κ (pair), are the atomic cross sections (cm²/atom) multiplied by atoms/cm³ of material and have

dimensions of cm^{-1}. Mass attenuation coefficients are the linear coefficients (cm^{-1}) divided by the density ρ (g/cm^3), thus σ/ρ, τ/ρ, κ/ρ, with dimensions of cm^2/g, and have the advantage of being independent of the actual density and physical state of the attenuator. Each mass attenuation coefficient for an element is the corresponding atomic cross section multiplied by the number of atoms per gram (Avogadro's number/atomic weight). Compton mass attenuation coefficients are nearly independent of Z because the number of electrons per gram varies only slightly among all elements except hydrogen.

The total *mass attenuation coefficient* μ_0/ρ is the sum of Compton absorption (σ_a/ρ), Compton scattering (σ_s/ρ), photoelectric attenuation (τ/ρ), and pair-production attenuation (κ/ρ),

$$\frac{\mu_0}{\rho} = \frac{\sigma_a}{\rho} + \frac{\sigma_s}{\rho} + \frac{\tau}{\rho} + \frac{\kappa}{\rho} = \frac{\sigma}{\rho} + \frac{\tau}{\rho} + \frac{\kappa}{\rho} \tag{8e-34}$$

In some narrow-beam attenuation situations a portion of the coherent, elastic Rayleigh scattering may also be effective.

The *mass absorption coefficient* relates only to the actual absorption of photon energy. This is a two-step process involving, first, the conversion of photon energy to kinetic energy of secondary electrons and to rest energy of electron pairs and, second, the dissipation of this kinetic energy mainly by ionization and excitation of the atoms in the absorbing medium, but to a small extent also by bremsstrahlung from radiative collisions of the secondary electrons with atomic nuclei in the absorber. There is no ambiguity about the first step, but the variety of treatments of the second step has led to a confusing group of absorption coefficients, including the so-called "true-absorption," "real-absorption," "energy-absorption," "dose-absorption," and "energy-transfer-absorption" coefficients.

If a collimated beam containing n photons/cm^2 sec, each having energy $h\nu_0$ MeV, is normally incident on an absorber of thickness dx and density ρ, then the number dn of photons/cm^2 sec which will have collisions is

$$dn = n\mu_0\, dx = n\left(\frac{\mu_0}{\rho}\right)(\rho\, dx) \tag{8e-35}$$

The incident photon *intensity* is $I = nh\nu_0$ MeV/cm^2 sec, and the energy transferred from incident photons to secondary electrons, which is closely similar to the "absorbed dose rate" in MeV/g sec, can be written as

$$dI = nh\nu_0\left(\frac{\mu_{aben}}{\rho}\right)(\rho\, dx) \qquad \frac{\text{MeV}}{\text{cm}^2\,\text{sec}} \tag{8e-36}$$

or

$$\frac{dI}{\rho\, dx} = I\left(\frac{\mu_{aben}}{\rho}\right) \qquad \frac{\text{MeV}}{\text{g sec}} \tag{8e-37}$$

where dI is the change in the intensity of the photons, and the mass-absorption coefficient (μ_{aben}/ρ) can be defined in a variety of slightly different ways.

Most generally one can write

$$\frac{\mu_{aben}}{\rho} \equiv \left(\frac{\sigma}{\rho}\right) f_c + \left(\frac{\tau}{\rho}\right) f_\tau + \left(\frac{\kappa}{\rho}\right) f_\kappa \tag{8e-38}$$

where the dimensionless factors f_c (Compton), f_τ (photo), and f_κ (pair) represent the fraction of the incident photon energy $h\nu_0$ which is considered to be absorbed in the medium from each type of interaction. The size of the "region of interest" relative to the mean free path of the secondary photons in the medium plays an important role in the choice of these dimensionless factors.

The situation is clearest for the Compton interaction. The energy of the Compton scattered photon is usually large enough to permit it to escape from a small "region

of interest" without interacting. Then the photon energy transferred to electrons is simply the kinetic energy acquired by the Compton recoil electron. Then, by Eq. (8e-30)

$$f_c = \frac{T_{av}}{h\nu_0} = \frac{\epsilon\sigma_a}{\epsilon\sigma} = \frac{\sigma_a/\rho}{\sigma/\rho} \tag{8e-39}$$

Hence

$$\left(\frac{\sigma}{\rho}\right) f_c = \frac{\sigma_a}{\rho} = \frac{\sigma}{\rho} - \frac{\sigma_s}{\rho} \tag{8e-40}$$

or just the Compton mass absorption coefficient σ_a/ρ.

In the photoelectric interaction the kinetic energy of the ejected photoelectron is, by Eq (8e-32), $T = h\nu_0 - B_e$; hence one extreme estimate of f_r is

$$(f_r)_1 = \frac{T}{h\nu_0} = \frac{h\nu_0 - B_e}{h\nu_0} \tag{8e-41}$$

which would be valid if the binding energy B_e is not released as electron kinetic energy in the volume of interest. However the excitation energy B_e may be emitted as Auger electrons or as K, L, M, . . . X-ray photons. When it is emitted as Auger electrons, the energy B_e is locally present in the medium as kinetic energy of electrons and $f_r = 1$. When B_e is emitted as X rays, these photons are somewhat analogous to a Compton scattered photon and could be excluded from f_r. If Φ is the average fluorescence yield [Φ increases with Z, rising from 0.01 for $Z = 10$ (Ne) to about 0.4 for $Z = 29$ (Cu) and 0.95 for $Z = 82$ (Pb)], then another estimate of f_r is

$$(f_r)_2 = \frac{h\nu_0 - \Phi B_e}{h\nu_0} = 1 - \frac{\Phi B_e}{h\nu_0} \tag{8e-42}$$

The correction term $\Phi B_e/h\nu_0$ is negligible for light elements because Φ is so small. For heavy elements, where Φ approaches unity, $\Phi B_e/h\nu_0$ is comparable to unity for photon energies near the absorption edge (K edge = 0.088 MeV in Pb), then decreases in importance as $h\nu_0$ increases. But the fluorescence radiation has a very short mean free path (for example, 0.06 cm in Pb) and is therefore reabsorbed very close to the emitting atom. The correction $\Phi B_e/h\nu_0$ is therefore justifiable only if the "volume of interest" for energy absorption is very small, for example, less than 1 mm³ in Pb. Therefore, in absorbers having an appreciable thickness the energy B_e is all reabsorbed in a small volume and the effective value of f_r would be

$$(f_r)_3 = 1 \tag{8e-43}$$

In the pair-production interaction, the total kinetic energy of the electron pair (or of the triplet in the case of pair production in the field of an atomic electron) is $h\nu_0 - 2m_0c^2$. Hence the fraction of $h\nu_0$ which appears at once as kinetic energy of secondary electrons is

$$(f_\kappa)_1 = \frac{h\nu_0 - 2m_0c^2}{h\nu_0} = 1 - \frac{2m_0c^2}{h\nu_0} = 1 - \frac{2}{\alpha} \tag{8e-44}$$

The energy $2m_0c^2$ is reemitted as two 0.511-MeV annihilation photons at the point of annihilation of the positron member of the electron pair. This annihilation radiation is the analog of Compton scattered radiation. In Pb, it has a mean free path of about 0.6 cm. For absorbers whose dimensions are small, the annihilation radiation clearly plays the role of a scattered radiation and should be so treated as in $(f_\kappa)_1$. For larger absorbers it has been a common approximation to ignore this correction term for annihilation radiation and to take

$$(f_\kappa)_2 = 1 \tag{8e-45}$$

This approximation usually introduces only a small change in μ_{aben}/ρ even for thin absorbers of heavy elements because at modest energies, say 1 to 3 MeV, the pair-production interaction is only a small component of the total absorption while at very large photon energies, where the pair production is predominant, the correction $2m_0c^2/h\nu_0$ becomes small. The magnitude of the correction is shown in Figs. 8e-6 through 8e-11.

For certain dosimetric applications in radiological physics (see chap. 1 of ref. A1 for details) a value of μ_{aben}/ρ is utilized which includes only the kinetic energy transferred to charged particles per unit mass of irradiated material in an infinitesimally small

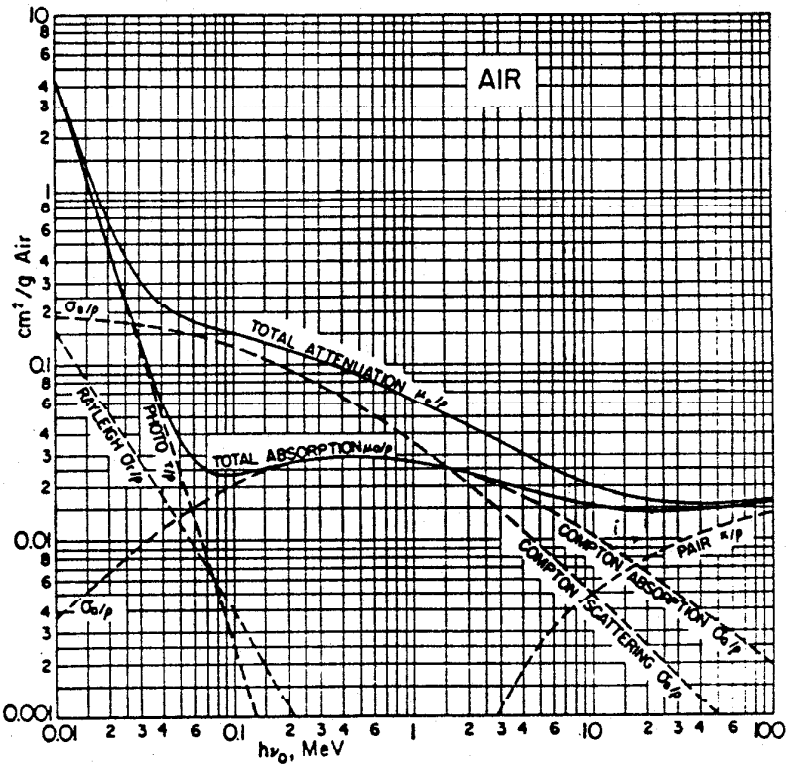

FIG. 8e-6. Mass attenuation coefficients for photons in "air" taken as 78.04 volume percent nitrogen, 21.02 volume percent oxygen, and 0.94 volume percent argon. At 0°C and 760 mm Hg pressure, the density of air is $\rho = 0.001293$ g/cm³. [*From Evans* (E1).]

region. This kinetic energy per unit mass has been named *kerma* (an acronym for *k*inetic *e*nergy *r*eleased in *ma*terial) by the ICRU (ref I1). The corresponding value of μ_{aben}/ρ received in 1962 (ref. I1) an "official" ICRU symbol and name (μ_K/ρ), the *mass energy-transfer coefficient*. For this particular special case of μ_{aben}/ρ, applicable under carefully specified conditions (ref. A1) to very small volumes of absorber, Eq. (8e-38) becomes

$$\frac{\mu_K}{\rho} = \frac{\sigma_a}{\rho} + \frac{\tau}{\rho}\left(1 - \frac{\Phi B_e}{h\nu_0}\right) + \frac{\kappa}{\rho}\left(1 - \frac{2m_0c^2}{h\nu_0}\right) \qquad \text{(8e-46)}$$

Tables of μ_K/ρ are given in refs. E4 and H3. For light elements and mixtures such as water, air, and Al, μ_K/ρ is substantially equal to μ_a/ρ of Eq. (8e-48) from 0.01 to 10 MeV.

For certain other dosimetric applications in radiological physics (chap. 1 of ref. A1), in which only the dissipation of electron kinetic energy by ionization and excitation

is considered, the bremsstrahlung losses by each type of secondary electron are deducted in the individual terms of Eq. (8e-46) which make up μ_K/ρ. The bremsstrahlung spectrum is heavily weighted with soft photons whose mean free path in the absorber usually will be small. However, for very high energy photons in heavy elements some of the higher-energy bremsstrahlung photons may have greater mean free paths than the primary photons. When the mass energy-transfer coefficient (μ_K/ρ) is reduced to account for bremsstrahlung losses by the secondary Compton, photoelectric, and pair electrons, the resulting coefficient is now called officially (ref. I1) the *mass energy-absorption coefficient* (μ_{en}/ρ). Note that μ_{en}/ρ depends upon the material with which the photon interacts within the infinitesimal "region of interest," as does μ_K/ρ in Eq. (8e-46), but in addition μ_{en}/ρ depends upon the atomic

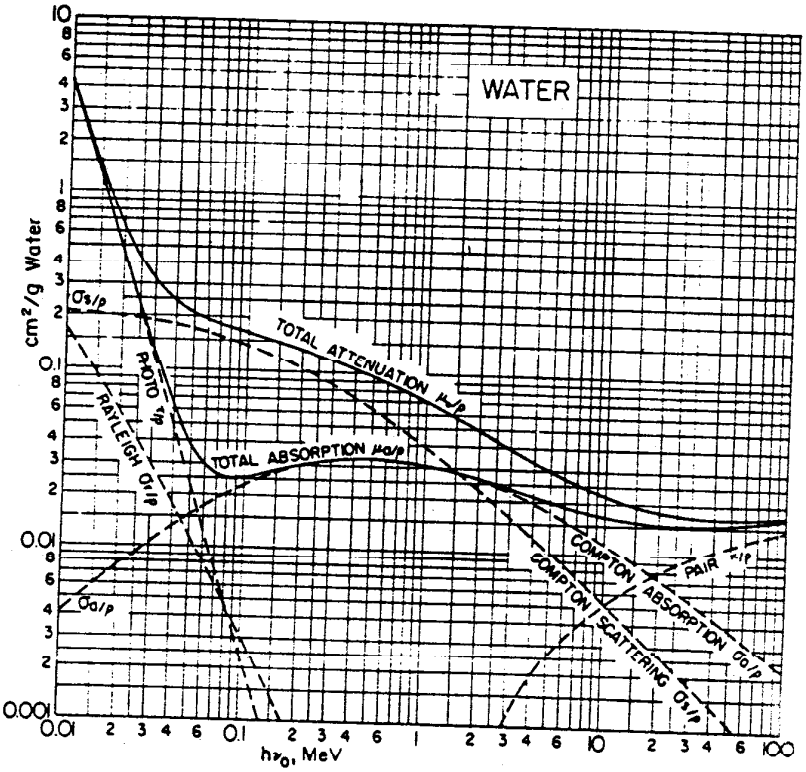

FIG. 8e-7. Mass attenuation coefficients for photons in water. [*From Evans* (E1).]

number of the material through which the secondary electron travels. Existing tables of μ_{en}/ρ are based on the assumption that the secondary electrons are absorbed in the same material in which they were formed. Bremsstrahlung losses by fast tertiary electrons produced in hard collisions by the Compton, photo, and pair electrons are usually ignored in computations of μ_{en}/ρ. Then for 2-MeV photons μ_{en}/ρ is less than μ_K/ρ by about 1 percent in Al, and about 7 to 8 percent in Pb or U. In order to use either μ_K/ρ or μ_{en}/ρ for computations of energy absorption or "absorbed dose," it is necessary to specify completely the spectrum of photon flux density, including all primary, secondary, tertiary, etc., photons, passing through the region of interest. The mass energy-absorption coefficient was first defined by Fano (ref. F2) in 1953, and the 1961 tables of μ_{en}/ρ by R. T. Berger (ref. B5) were called "mass energy-transfer" coefficients just before the name "mass energy-absorption coefficient" became official for μ_{en}/ρ in 1962 (ref. I1). Extensive tables of μ_{en}/ρ as well as μ_K/ρ are given in refs. E4 and H3.

We have noted that the mean free path of the secondary photons often is small. Hence for many practical cases involving absorbers of small to moderate size, we can select $(f_T)_2$ and $(f_\kappa)_1$ and write

$$\frac{\mu_{abs}}{\rho} = \frac{\sigma_a}{\rho} + \frac{\tau}{\rho} + \frac{\kappa}{\rho}\left(1 - \frac{2m_0c^2}{h\nu_0}\right) \tag{8e-47}$$

or, using $(f_\kappa)_2$, the common but approximate expression, usually called the *mass absorption coefficient* μ_a/ρ, given by

$$\frac{\mu_a}{\rho} = \frac{\sigma_a}{\rho} + \frac{\tau}{\rho} + \frac{\kappa}{\rho} \tag{8e-48}$$

The *mass absorption coefficient* (μ_a/ρ) is a slightly more general concept than either the mass energy-transfer coefficient (μ_K/ρ) or the mass energy-absorption coefficient (μ_{en}/ρ); both the latter are special cases of μ_a/ρ designed for the computation of radiation dose or dose rate in infinitesimally small volumes of absorbing material. Tables of μ_a/ρ as well as μ_K/ρ and μ_{en}/ρ for 18 elements from H to U over the energy range 0.01 to 10 MeV are given in ref. H3.

Figures 8e-6 through 8e-11 give the mass attenuation coefficients μ_0/ρ of Eq. (8e-34) and the mass absorption coefficients μ_a/ρ of Eq. (8e-48) and (dashed) μ_{abs}/ρ of Eq.

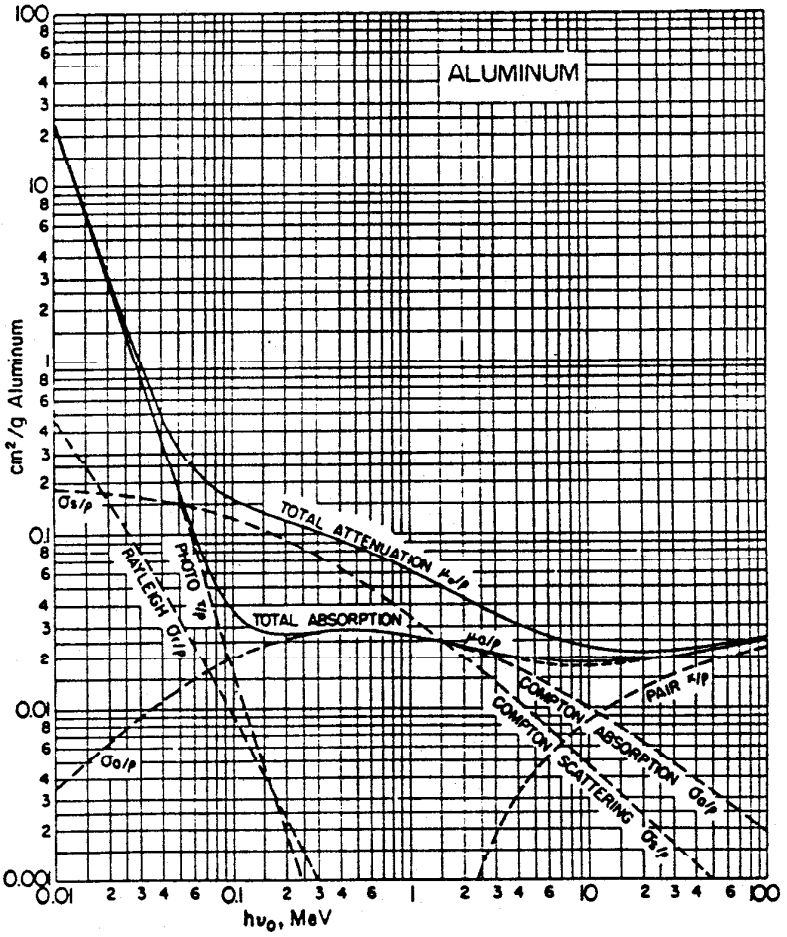

FIG. 8e-8. Mass attenuation coefficients for photons in aluminum ($Z = 13$). The dashed branch on the μ_a/ρ curve shows the effect of excluding annihilation photons [Eq. (8e-47)]. The corresponding linear coefficients for aluminum may be obtained by multiplying all curves by $\rho = 2.70$ g/cm³ Al. [*From Evans* (E1).]

(8e-47) for air, water, Al, Cu, NaI, and Pb from refs. E1 and E2 as computed from the tables in ref. W1 of the collision cross sections per atom for photoelectric interactions, pair-production interactions, and coherent scattering and from the tables for σ, σ_a, and σ_s in ref. E2. The pair-production coefficients include the effects of the atomic electrons. The curves marked "total absorption" are $(\mu_a/\rho) = (\sigma_a/\rho) + (\tau/\rho) + (\kappa/\rho)$, where σ_a, τ, and κ are the corresponding linear coefficients for Compton absorption,

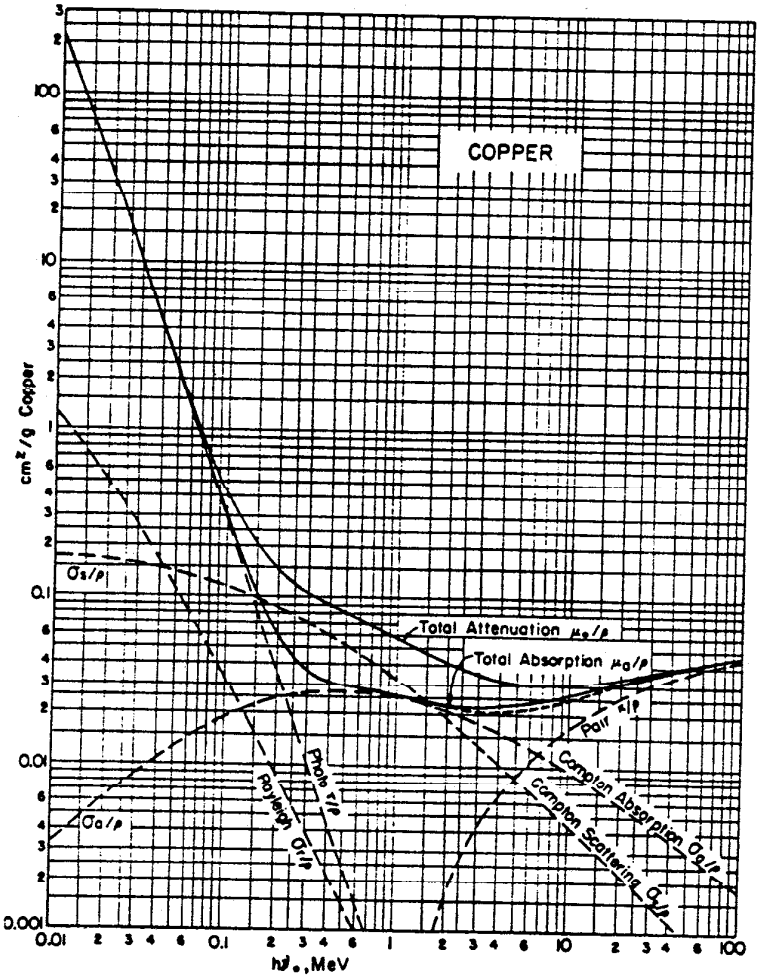

FIG. 8e-9. Mass attenuation coefficients for photons in copper ($Z = 29$). The dashed branch on the μ_a/ρ curve shows the effect of excluding the annihilation photons [Eq. (8e-47)]. The corresponding linear coefficients for copper may be obtained by multiplying all curves by $\rho = 8.92$ g/cm³ Cu. [*From Evans* (E2).]

photoelectric collisions, and pair-production collisions. When the Compton scattering coefficient σ_s is added to μ_a, we obtain the curves marked "total attenuation," which are $(\mu_0/\rho) = (\mu_a/\rho) + (\sigma_s/\rho)$. The total Rayleigh scattering cross section (σ_r/ρ) is shown separately and is estimated by deducting the Compton collision cross section σ of ref. E2 from the total coherent cross sections of ref. W1. Because the Rayleigh scattering is elastic and is confined to small angles, it has not been included in μ_0/ρ.

A dashed branch on the mass-absorption-coefficient curves μ_a/ρ in the vicinity of 2 to 30 MeV shows the effect of correcting the κ/ρ contribution for annihilation radi-

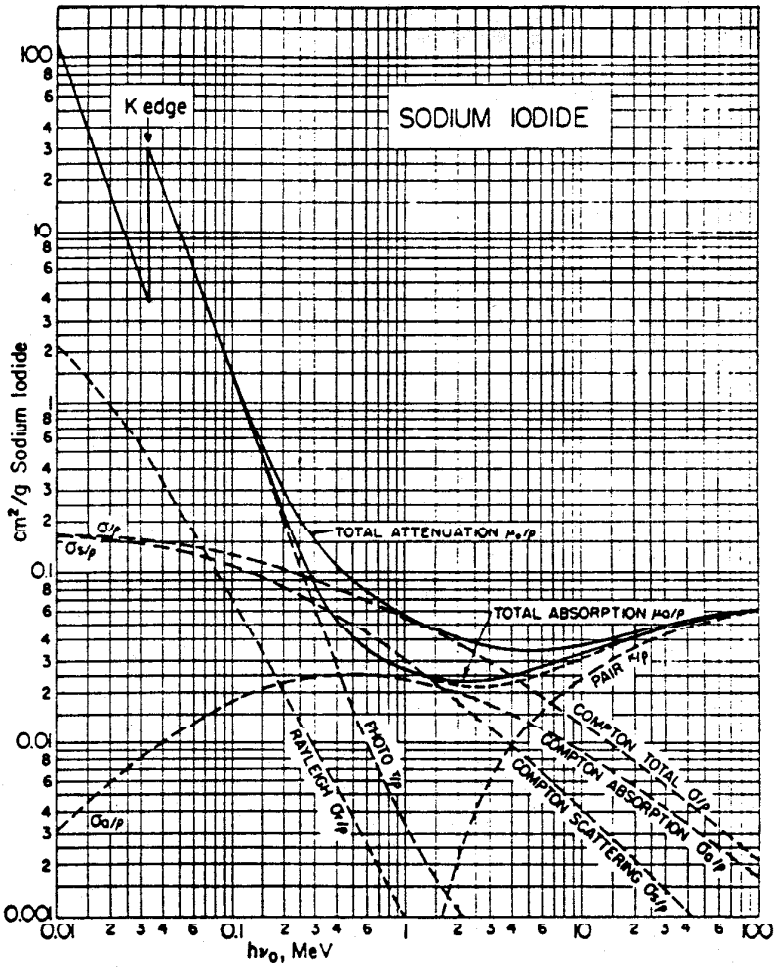

FIG. 8e-10. Mass attenuation coefficients for photons in pure NaI. The "Compton total" attenuation coefficient $(\sigma/\rho) = (\sigma_a/\rho) + (\sigma_s/\rho)$ is shown explicitly, because of its usefulness in predicting the behavior of NaI(Tl) scintillators. The 0.1 to 0.2 percent thallium activator in NaI(Tl) scintillators is ignored here. The dashed branch on the μ_a/ρ curve shows the effect of excluding annihilation photons [Eq. (8e-47)]. Linear attenuation coefficients for NaI may be obtained using $\rho = 3.67$ g/cm³ NaI. [*From Evans* (E1).]

ation in accord with Eq. (8e-47). This correction has a maximum value of about 12 percent for Pb between 3 and 8 MeV and decreases with atomic number. The correction is too small (<3 percent) to be visible on the curves for water and air.

Mixtures and Compounds. An absorber whose bulk density is ρ and which is made up of a mixture of elements whose mass attenuation (or absorption) coefficients are (μ_1/ρ_1), (μ_2/ρ_2), . . . will have an over-all mass attenuation coefficient given by

$$\frac{\mu}{\rho} = \frac{\mu_1}{\rho_1} w_1 + \frac{\mu_2}{\rho_2} w_2 + \cdots \tag{8e-49}$$

where w_1, w_2, . . . are the fractions by weight of the elements which make up the absorber. This relationship is valid when all the (μ/ρ)'s represent total attenuation coefficients, total absorption coefficients, or any one or more partial (Compton, photo, pair) effects. Because the chemical binding energies between atoms in a molecule are very small, chemical compounds are treated as mixtures.

Interpolation Formulas. To obtain corresponding coefficients for other elements, use a graph for a nearby elementary substance (Al, Cu, or Pb), and the following relationships:

1. Comptom absorption, scattering, or collision coefficients:

$$\frac{\sigma_1}{\rho_1} = \frac{\sigma_2}{\rho_2}\frac{A_2}{A_1}\frac{Z_1}{Z_2} \tag{8e-50}$$

where Z is atomic number, A is atomic weight, and the subscripts 1 and 2 refer to any two elements.

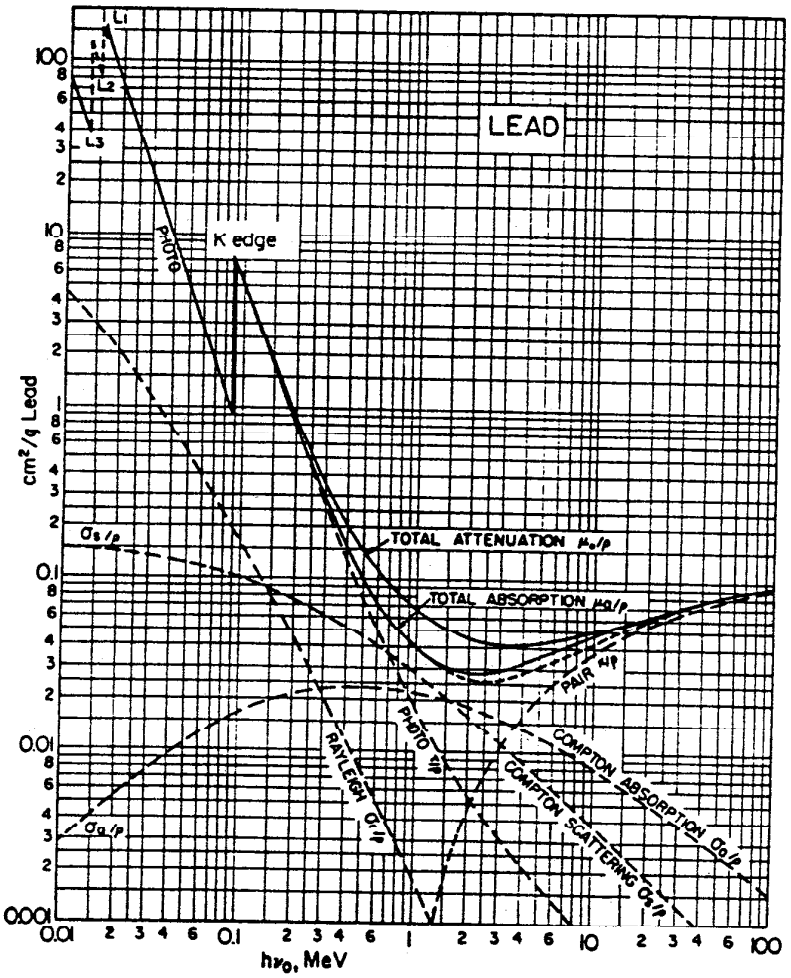

FIG. 8e-11. Mass attenuation coefficients for photons in lead. The dashed branch on the μ_a/ρ curve shows the effect of excluding annihilation photons [Eq. 8e-47)]. The corresponding linear coefficients for lead may be obtained using $\rho = 11.35$ g/cm³ Pb. [*From Evans* (E1).]

2. Photoelectric attenuation coefficients:

$$\frac{\tau_1}{\rho_1} = \frac{\tau_2}{\rho_2}\frac{A_2}{A_1}\left(\frac{Z_1}{Z_2}\right)^n \tag{8e-51}$$

where the exponent n is an empirical function of $h\nu$ as given in Fig. 8e-12.

3. Pair-production attenuation coefficients, screening neglected:

$$\frac{\kappa_1}{\rho_1} = \frac{\kappa_2}{\rho_2}\frac{A_2}{A_1}\left(\frac{Z_1}{Z_2}\right)^2 \tag{8e-52}$$

8e-6. Interpretation of Scintillation Spectrometer Pulse-height Spectra. Incident monoenergetic photons produce secondary electrons of many energies T. The scintillations from these electrons therefore give a continuous distribution of pulse heights. This distribution is further broadened by statistical fluctuations (see ref. B4) in the actual light-pulse output from every monoenergetic subgroup of electrons, such as the photoelectrons.

Figure 8e-13 is a typical pulse-height spectrum, characteristic of an NaI(Tl) scintillator in the size range of 2 by 2 to 4 by 4 in., irradiated by the 0.662-MeV γ rays emitted in the decay of Cs^{137}. Pulses in the *total energy peak* arise whenever the total energy $h\nu$ of one photon is absorbed in the scintillator and include a primary photoelectric event accompanied by absorption within the scintillator of the resulting X rays and Auger electrons, a primary Compton event accompanied by absorption also of the Compton scattered photon, and in the case of $h\nu > 1.02$ MeV a primary pair-production event followed by absorption of both quanta of annihilation radiation.

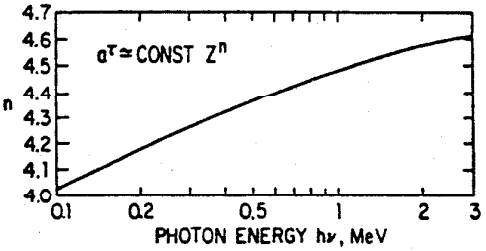

FIG. 8e-12. Approximate variation of the photoelectric cross section $_a\tau$ cm²/atom with Z^n, for various values of $h\nu$. For use with the interpolation formula [Eq. (8e-51)]. [*By N. C. Rasmussen, from Evans* (E1).]

Escape peaks are present also at energies of $h\nu - 28$ keV when the K_α X ray of iodine is not absorbed and at $h\nu - 511$ keV and $h\nu - 1{,}022$ keV when one or both annihilation photons are not absorbed in the crystal.

The *resolution* of the spectrometer is usually described as the full width at half maximum of the total energy peak, divided by the total energy, and is commonly of the order of 8 percent for 0.662-MeV γ rays in 4- by 4-in. NaI(Tl) crystals. For a given crystal and photomultiplier the width of the total energy peak increases roughly as $\sqrt{h\nu}$; hence the percent resolution varies roughly as $1/\sqrt{h\nu}$.

The Compton edge in Fig. 8e-13 is the high-energy end of the Compton recoil-electron distribution of Fig. 8e-5 and of Eq. (8e-21), broadened out somewhat by multiple Compton collisions in the crystal and by the same type of inherent statistical fluctuations which produce the width of the total energy peak (see ref. B4). The energy of the Compton edge is, by Eq. (8e-9),

$$T_{max} = h\nu_0 \frac{2\alpha}{1 + 2\alpha} = h\nu_0 - (h\nu')_{min} \tag{8e-53}$$

The *backscatter peak* is an unwanted "ghost line" produced by photons which have been scattered into the scintillator from surrounding materials. These are mainly Compton large-angle backscattered photons; hence their energy and that of the backscatter peak which arises from their total absorption in the crystal are, by Eq. (8e-6), just slightly greater than

$$(h\nu')_{min} = m_0c^2 \frac{\alpha}{1 + 2\alpha} \tag{8e-54}$$

Figure 8e-3 contains a plot of $h\nu'$ for $\vartheta = 180$ deg, which is $(h\nu')_{min}$, and hence gives the minimum energy $(h\nu')_{min}$ of the backscatter peak and also the energy separation $(h\nu_0 - T_{max}) = (h\nu')_{min}$ between the total energy peak $(h\nu_0)$ and the Compton edge T_{max}. The center of gravity of the backscatter peak is usually at an energy greater than $(h\nu')_{min}$ because photons which have been scattered through less than $\vartheta = 180$ deg are strongly involved. For many experimental situations the effective backscatter angle is between $\vartheta = 120$ and 150 deg, for which $h\nu'$ is also given in Fig. 8e-3.

The *intrinsic efficiency* (or interaction ratio) of a NaI(Tl) crystal is the total number of pulses under the entire pulse-height distribution curve (excluding the backscatter pulses) per primary photon incident on the crystal face. The intrinsic efficiency, as well as the pulse-height distribution, depends upon the geometry of source and crystal and has been calculated by Monte Carlo methods for several arrangements (see refs. B1, B2, and M1) using the collision cross sections and total mass attenuation coeffi-

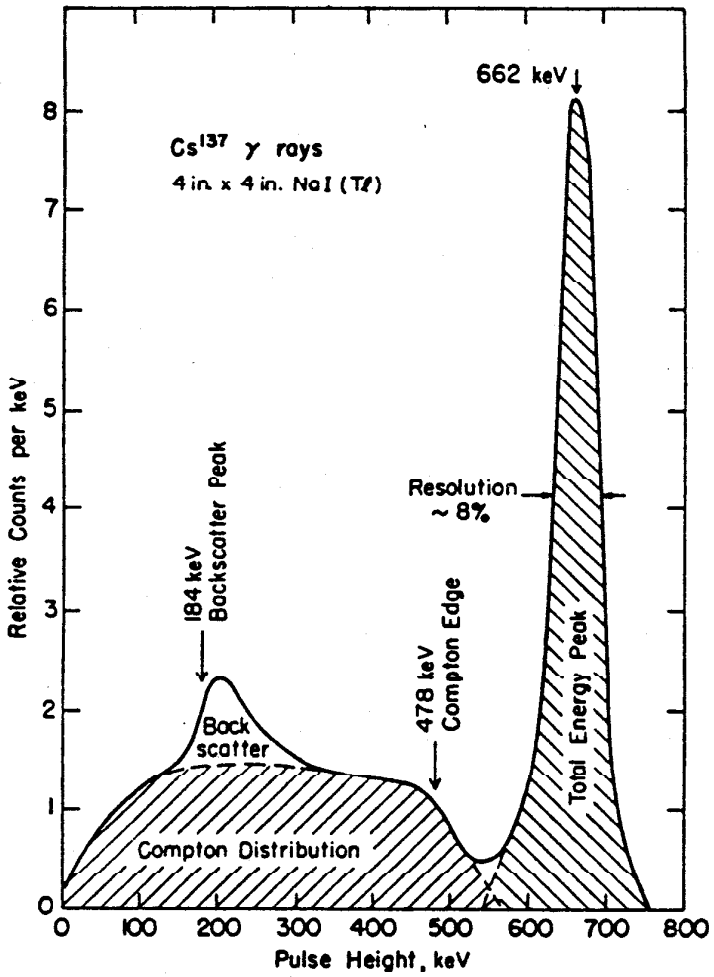

FIG. 8e-13. Typical pulse-height distribution in a 4 in. × 4 in. NaI(Tl) scintillator irradiated by 0.662-MeV γ rays from the decay of Cs^{137}. The resolution is about 8 percent of the energy of the total-energy peak. For $h\nu_0 = 662$ keV, $(h\nu')_{min} = 184$ keV, and $T_{max} = 478$ keV as marked.

cients for NaI as given in Fig. 8e-10. The minor effect of the 0.1 to 0.2 percent thallium content of NaI(Tl) is generally ignored. Calculations have been made by the same methods of the so-called *photofraction*, which is the ratio of the number of pulses under the total energy peak to the total number of pulses in the entire distribution (excluding the backscatter peak because it is not due to primary photons and depends on the experimental arrangement). Note that the photofraction includes pulses arising from all total absorption mechanisms and thus exceeds the effect of photoelectric collisions.

Figure 8c-14 gives illustrative values of the *intrinsic efficiency* and of the *photofraction* for some common sizes of NaI(Tl) crystals irradiated by monoenergetic photons from a point source placed along the extended cylindrical axis of the crystal, according to calculations at five γ-ray energies from 0.279 to 4.45 MeV by Miller, Reynolds, and Snow (ref. M1; for other geometries and crystal sizes see refs. M1, B1, B2).

Especially when a number of primary photon energies are present, the interpretation of a pulse-height distribution may become very complicated and dependent upon the preparation of a response matrix and an *inversion matrix* for the particular geometry and scintillator (see ref. H2).

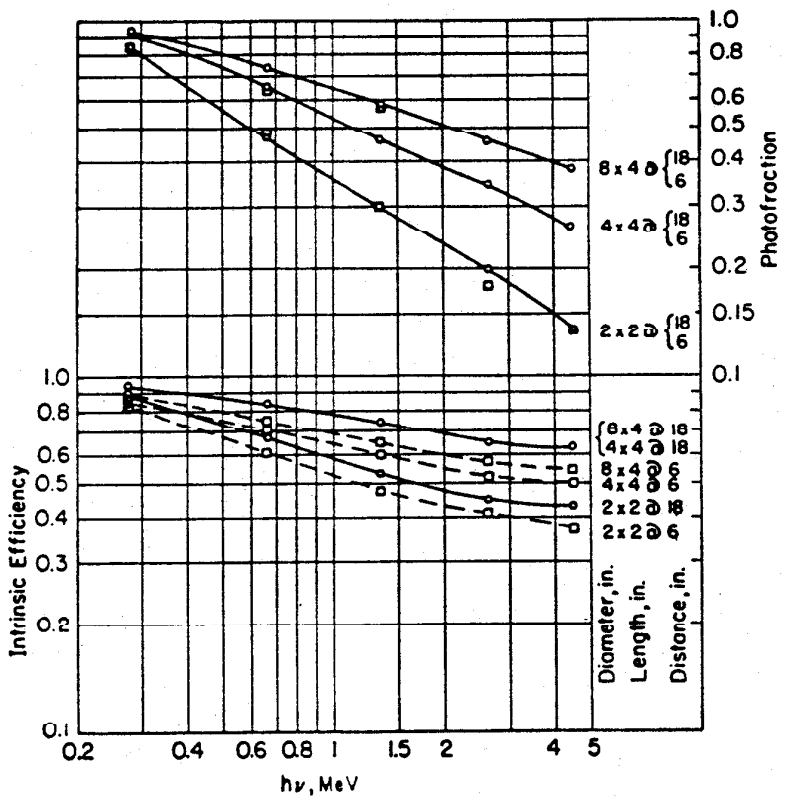

FIG. 8e-14. Illustrative calculated values of the *photofraction* (pulses in total-energy peak/pulses in entire distribution) and the *intrinsic efficiency* (pulses per photon striking the crystal face) for point sources of γ rays located on the axis of a NaI(Tl) crystal at 18 in. (circles) or 6 in. (squares) from the crystal face, for crystals whose diameters and lengths in inches are shown opposite the curves.

Germanium semiconductor γ-ray detectors have much higher resolution than NaI(Tl) scintillators but thus far are available only in relatively small sizes and must be operated at greatly reduced temperatures. The individual interaction coefficients for photons in germanium (Z = 32) are not included in most primary tables, but can be computed by interpolation from nearby elements such as copper (Z = 29). The Compton, photoelectric, and pair-production coefficients for germanium, from 0.05 to 10 MeV, have been computed by Chapman (see ref. C1).

8e-7. Self-absorption in γ-ray Sources. There is appreciable self-absorption in substantially all practical γ-ray sources, due to interactions suffered by primary photons while emerging from within the source. The common types of γ-ray standards used in most laboratories may have from 1 to 10 percent self-absorption. The

quantitative corrections for self-absorption depend strongly on the relative response of the detecting instruments to primary and to degraded photons (see refs. E1 and E3).

When the response of the detector is proportional to the γ-ray intensity (MeV/sec cm^2) and independent of the photon energy, when the distance between the source and detector is large compared with the dimensions of the source, and when the self-absorption is less than about 10 percent, a good approximation for the ratio of the net intensity I to the intensity I_0 in the absence of self-absorption is:

1. For radiation along the axis of a cylindrical source of length l:

$$\frac{I}{I_0} \simeq e^{-(\frac{1}{2})\mu_a l} \tag{8e-55}$$

2. For radiation normal to the axis of a cylindrical source of radius R:

$$\frac{I}{I_0} \simeq e^{-\left(\frac{8}{3\pi}\right)\mu_a R} \tag{8e-56}$$

3. For radiation from a spherical source of radius R:

$$\frac{I}{I_0} \simeq e^{-(\frac{2}{3})\mu_a R} \tag{8e-57}$$

In each case μ_a is the linear absorption (not attenuation) coefficient of the source material.

In the limiting case of very large γ-ray sources, whose dimensions are several mean free paths (1 mfp = $1/\mu_0$), the external γ-ray intensity is simply proportional to the solid angle subtended by the source at the position of the detector.

8e-8. Build-up Factor for Photons in Broad-beam Attenuation. In most practical situations in γ-ray and X-ray shielding or in energy absorption, a significant fraction of the scattered photons and the secondary photons can reach the detector. Accurate calculation of the spectral distribution and intensity of the scattered and secondary photons in these "poor geometry" or "broad-beam" situations is often extremely complicated. The status of extensive theoretical and experimental work at the National Bureau of Standards and elsewhere is admirably summarized as of 1958 in ref. F3.

The transmitted intensity of *primary* photons can be calculated easily, using the total attenuation coefficient μ_0, because *the primary radiation is always in good geometry*. The complicated contribution of scattered and secondary photons is described by the so-called *build-up factor*, which is the ratio of the observed effect to the effect produced only by the residual primary radiation. Thus there are different build-up factors for photon intensity or energy flux, photon number, dose rate in an air cavity, and energy absorption in the medium (see ref. G1). The build-up factor B for dose rate is defined as

$$\begin{aligned} B &\equiv \frac{\text{total observed dose rate}}{\text{primary dose rate}} \\ &= 1 + \frac{\text{dose rate due to scattered and secondary radiation}}{\text{dose rate due to primary radiation}} \end{aligned} \tag{8e-58}$$

The ratio of the dose rate from secondaries dP_{sec} to dose rate from primaries dP_{prim}, and hence the build-up factor B, is found experimentally and theoretically (see ref. G1) to increase monotonically with the thickness r of absorbing material. Thus "equilibrium" between secondary and primary photons is never reached. To a reasonable approximation, especially for the dose rate measured inside an effectively

infinite medium at a distance r from a point source in the medium, the increase of B with r can be represented by

$$B = 1 + \frac{dP_{sec}}{dP_{prim}} = 1 + a(\mu_0 r)^k \tag{8e-59}$$

where $\mu_0 r$ is the distance r from the source measured in mean free paths of the primary radiation and k is a constant which depends upon the photon energy $h\nu$ of the photons

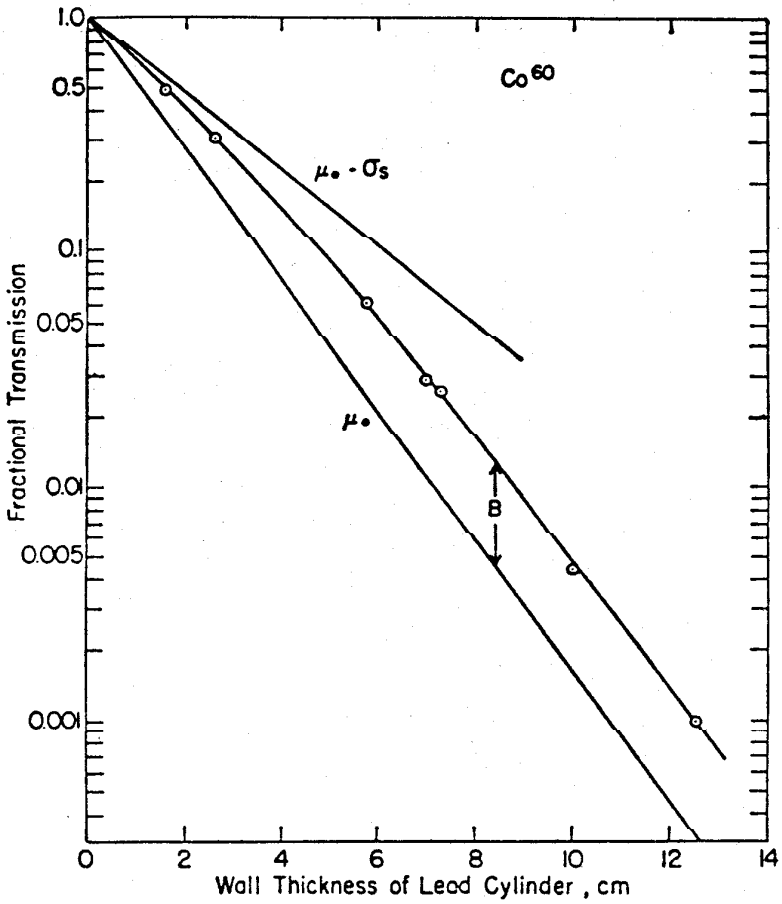

FIG. 8e-15. Transmission of Co^{60} γ rays through cylindrical Pb shields. Theoretical lines for the transmission of undeflected primary photons (μ_0) and for the absorption of primary energy ($\mu_0 - \sigma_s = \mu_a$) are shown for comparison. The ratio of the experimentally observed exposure dose rate outside the shield to the theoretical dose rate due to transmitted primary photons (μ_0) is the dose-rate build-up factor, marked B. [*Data by A. Morrison, from Evans* (E1).]

and the atomic number Z of the absorber (see refs. F1 and P1) and is of the order of unity. The proportionality constant a can be shown (see ref. E1) from conservation of energy to be

$$a = \frac{1}{\Gamma(k+1)} \frac{\sigma_s}{\mu_a} \tag{8e-60}$$

where $\Gamma(k+1)$ is the gamma function of $k+1$; hence $\Gamma(k+1) = k!$ whenever k is an integer. The linear Compton scattering coefficient σ_s, the linear absorption coefficient σ_a, and the linear attenuation coefficient $\mu_0 = \mu_a + \sigma_s$ are each evaluated for the *primary* photon energy in the medium.

An oversimplified but useful approximate theory (see ref. E1) for γ-ray energies in the neighborhood of 1 MeV and for low or medium Z results when k is taken as unity; then

$$B \simeq 1 + \frac{\sigma_s}{\mu_a}(\mu_0 r) \tag{8e-61}$$

The effects of boundaries (see refs. F3 and E1) and hence the build-up factor for radiation measured outside a shield, rather than inside the shielding material, are much more difficult to approach theoretically and are now mainly empirical.

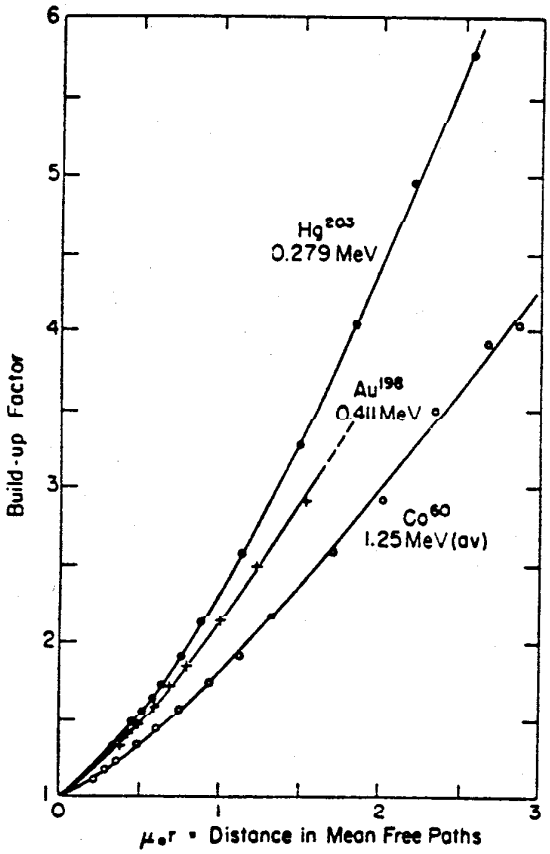

FIG. 8e-16. Build-up factors for point sources of γ rays of three energies measured in an essentially infinite water medium. [*Data by M. A. Van Dilla, from Evans* (E1).]

Figure 8e-15 illustrates the γ-ray dose rate measured outside a Pb shield surrounding a Co^{60} source and the physical meaning of the dose-rate build-up factor B.

Figure 8e-16 illustrates the monotonic increase of the dose-rate build-up factor inside a large water medium with distance from point sources of 1.25, 0.411, and 0.279-MeV γ rays.

8e-9. Gamma-ray Output of Radionuclides. Many radionuclides emit γ rays and can be used as photon sources. It is convenient to describe the source strength of a particular radionuclide in terms of the so-called *specific γ-ray constant*, Γ, which is defined as the exposure dose rate in milliroentgens (mR) per hour produced in air at a distance of one meter from a point source of one millicurie (mCi) of the radionuclide. The exposure dose rate has usually been taken as equivalent to $I(\mu_a/\rho)$, where I is the γ-ray intensity (MeV/cm^2 sec), and μ_a/ρ is the mass absorption coeffi-

cient of air for the particular photon energy involved [see Eqs. (8e-37) and (8e-48)]. Inserting the geometrical factors, and omitting any attenuation of the γ rays in 1 meter of air, the specific γ-ray constant becomes

$$\Gamma = 19.3 \sum_i n_i (h\nu)_i \left(\frac{\mu_a}{\rho}\right)_i \quad \frac{\text{mR}}{\text{mCi} \cdot \text{hr}} \text{ at 1 meter} \tag{8e-62}$$

where n_i photons of energy $(h\nu)_i$ are emitted per disintegration, and the average energy to form one ion pair in air has been taken as $W = 34.0$ eV per ion pair. Because μ_a/ρ for air varies only slightly (+15 percent over the usual domain of nuclear γ-ray energies (see Fig. 8e-6), a convenient approximate rule is

$$\Gamma \approx \tfrac{1}{2} \Sigma(h\nu) \quad \text{mR/mCi} \cdot \text{hr at 1 meter} \tag{8e-63}$$

where $\Sigma(h\nu)$ is the total photon energy in MeV emitted per disintegration.

TABLE 8e-3. THE SPECIFIC γ RAY CONSTANT Γ IN MILLIROENTGENS PER HOUR PRODUCED AT 1 METER BY THE NUCLEAR γ RAYS AND THE ANNIHILATION RADIATION FROM 1 MILLICURIE OF THE RADIONUCLIDES LISTED*

Nuclide	Half period	mR / hr · mCi at 1 meter	Nuclide	Half period	mR / hr · mCi at 1 meter
Na^{22}	2.58 yr	1.23	As^{76}	26.5 hr	0.4
Na^{24}	15.0 hr	1.84	Br^{82}	35.3 hr	1.5
Al^{28}	2.30 min	0.85	I^{128}	25.0 min	0.017
Mn^{52}	5.7 days	1.85	I^{130}	12.5 hr	1.20
Mn^{54}	314 days	0.47	I^{131}	8.05 days	0.23
Fe^{59}	45 days	0.62	Cs^{137}	30 yr	0.31
Co^{58}	71 days	0.54	Ta^{182}	115 days	0.6
Co^{60}	5.26 yr	1.29	Au^{198}	64.8 hr	0.24
Cu^{64}	12.9 hr	0.12	Ra^{226}	1,620 yr	0.84†
Zn^{65}	245 days	0.26			

* Revised from Evans (p. 722 of ref. E1) using $W = 34$ eV per ion pair.

† With 0.5-mm Pt filtration. Γ for Ra^{226} is usually expressed in terms of mg instead of mCi, the accepted experimental value being 0.825 mR/hr · mg at 1 meter (ref. I2). One gram of Ra^{226} has 3.62×10^{10} disintegrations/sec; 1 Ci = 3.7×10^{10}/sec. Thus the experimental value can be expressed as 0.844 mR/hr · mCi, in good agreement with the tabulated value.

Table 8e-3 gives numerical values computed from Eq. (8e-62) for the specific γ-ray constant, or exposure dose rate produced by nuclear γ rays (plus the annihilation radiation in the case of positron emitters) at 1 meter from a 1-mCi point source of several common radionuclides. These values are in reasonable agreement with computed and experimental values compiled by Mann and others (ref. I2).

References

A1. Attix, F. H., and W. C. Roesch, eds.: "Radiation Dosimetry," vol. 1, 2d ed., Academic Press, Inc., New York, 1968. The current authoritative treatise on the fundamental principles of radiological physics; 8 chapters carefully edited and cross-referenced.

B1. Bell, P. R.: The Scintillation Method, in "Beta- and Gamma-ray Spectroscopy," pp. 133–164, Kai Siegbahn, ed., Interscience Publishers, Inc., New York, 1955. Review of basic principles and experimental methods. A permanently valuable intro-

duction to the later literature. The revised version of this article is J. H. Neiler, and P. R. Bell, in "Alpha-, Beta-, and Gamma-ray Spectroscopy," vol. 1, pp. 245–302, Kai Siegbahn, Ed., North-Holland Publishing Co., Amsterdam, 1965.

B2. Berger, M. J., and J. Doggett: Response Function of NaI(Tl) Scintillation Counters, *Rev. Sci. Instr.* **27**, 269 (1956), and *Natl. Bur. Standards J. Research* **56**, 355 (1956). Monte Carlo calculations of intrinsic efficiency and photofraction for several sizes (0.5 in. diameter by 0.5 in. long to 5 in. diameter by 9 in. long) NaI(Tl) crystals irradiated axially by collimated monoenergetic γ rays at six energies from 0.279 to 4.45 MeV.

B3. Bethe, H. A., and J. Ashkin: Penetration of Gamma Rays, in "Experimental Nuclear Physics," vol. I, pp. 304–349, E. Segre, ed., John Wiley & Sons, Inc., New York, 1953. Theory and graphs for Compton, photoelectric, and pair-production interactions.

B4. Breitenberger, E.: Scintillation Spectrometer Statistics, in "Progress in Nuclear Physics," vol. 4, pp. 56–94, O. R. Frisch, ed., Pergamon Press, London, 1955. Theory and some experimental results on line width and shape from scintillation counters, extensive bibliography.

B5. Berger, Rosemary T.: The X- or Gamma-ray Energy Absorption or Transfer Coefficient; Tabulations and Discussions, *Radiation Research* **15**, 1, 1961. Definitive summary of various types of absorption coefficients with tables of the mass energy $1 = 1$ absorption coefficients for 0.01-MeV to 10-MeV photons in water, air, and 14 elements from H to Cu.

C1. Chapman, G. T.: Gamma-ray Attenuation Coefficients for Germanium, *Nucl. Instr. Methods* **52**, 101 (1967). Tables and a graph of the Compton, photoelectric, and pair-production coefficients for germanium ($Z = 32$), computed by interpolation among five elements ($Z = 20$, 26, 29, 42, and 50) in the tables by G. White Grodstein (ref. G2).

D1. Davisson, C. M., and R. D. Evans: Gamma-ray Absorption Coefficients, *Revs. Mod. Phys.* **24**, 79 (1952). Review of theory and experimental results through 1951 on Compton, photoelectric, and pair-production interactions, with graphs or tables for 24-elements.

D2. Davisson, C. M.: Interaction of Gamma Radiation With Matter, in "Alpha-, Beta- and Gamma-ray Spectroscopy," pp. 37–78, 827–843, K. Siegbahn, ed., North-Holland Publishing Company, Amsterdam, 1965. A thorough review of the theory, with tables for 21 elements from H to U and 4 compounds or mixtures, for Compton, Rayleigh, photoelectric, pair-production, and total cross sections from 0.01 to 100 MeV. The numerical tables are utilized and updated by those in refs. E4 and H3.

E1. Evans, R. D.: "The Atomic Nucleus," McGraw-Hill Book Company, New York, 1955. Textbook and reference book on nuclear physics. Chapters 23, 24, and 25 deal with interaction of photons with matter; theory, experiment, applications, graphs, and bibliography.

E2. Evans, R. D.: Compton Effect, in "Handbuch der Physik," vol. XXXIV, pp. 218–298, S. Flügge, ed., Springer-Verlag OHG, Berlin, 1958. Theory and experimental results on all aspects of the Compton interaction for free and bound electrons, polarized and unpolarized photons, with 42 figures and 8 tables.

E3. Evans, R. D., and R. O. Evans: Studies of Self-absorption in Gamma-ray Sources, *Rev. Mod. Phys.* **20**, 305 (1948). Theory and experimental results for self-absorption in cylindrical standard sources, particularly of radium.

E4. Evans, R. D.: X-ray and Gamma-ray Interactions, in "Radiation Dosimetry," vol. 1, pp. 93–155, 2d ed., F. H. Attix and W. C. Roesch, eds., Academic Press, Inc., New York, 1968. An amended and enlarged version of the present chapter, plus extensive new tables of mass attenuation coefficients μ_0/ρ, mass energy-transfer coefficients μ_K/ρ, and mass energy-absorption coefficients μ_{en}/ρ for 22 elements from H to U and for 11 mixtures or compounds, prepared by J. H. Hubbell as an extension of ref. H3.

F1. Fano, U.: Gamma-ray Attenuation. Analysis of Penetration, *Nucleonics* **11**(9), 55 (1953). Summary of the progress to 1953 of the NDA-NBS program of calculation and measurement of multiple scattering, deep penetration, and build-up factors in infinite homogeneous media. See Goldstein and Wilkins (ref. G1) and Fano, Spencer, and Berger (ref. F3) for later developments.

F2. Fano, U.: Gamma-ray Attenuation. Basic Processes, *Nucleonics* **11**(8), 8 (1953). Review of photon interactions and qualitative description of corrections to the mass absorption coefficient, for fluorescence radiation, bremsstrahlung, and rest energy of electron pairs, to obtain energy-absorption coefficient μ_{en}. Table of μ_{en} from 0.088 to 10 MeV for water, Al, Fe, and Pb.

F3. Fano, U., L. V. Spencer, and M. J. Berger: Penetration and Diffusion of X Rays, in "Handbuch der Physik," vol. XXXVIII/2, pp. 660–817, S. Flügge, ed., Springer-

Verlag OHG, Berlin, 1959. The definitive treatise on multiple scattering, build-up factors, and related quantities in homogeneous infinite media and in bounded media, with 57 figures and 23 tables.

G1. Goldstein, H., and J. E. Wilkins, Jr.: Calculations of the Penetration of Gamma Rays, *U.S. Atomic Energy Comm. Rept.* NYO-3075, 1954, 196 pp. Theory and results of calculations of spectra of multiply scattered photons, build-up factors, and related quantities for monoenergetic 0.5- to 10-MeV γ-ray sources in infinite homogeneous media, by the "moments method" of Spencer and Fano; 140 tables and 75 graphs.

G2. Grodstein, G. W.: X-ray Attenuation Coefficients from 10 keV to 100 MeV, *Natl. Bur. Standards Circ.* 583, 1957, 54 pp. Review of theory of photon interactions, with some experimental comparisons. Tables of theoretical atomic cross sections for Compton interactions with and without coherence terms, photoelectric effect, and pair production by nuclear and by electronic interactions for 24 elements and five mixtures. A widely used basic reference. Earlier editions of these tables appeared (see ref. W1) under the same title by G. R. White as *Natl. Bur. Standards Rept.* 1003, 1952, and on pp. 857–874 of "Beta- and Gamma-ray Spectroscopy," Kai Siegbahn, ed., Interscience Publishers, Inc., New York, 1955. A supplement to Circular 583, 1959, under the same title, by R. T. McGinnies, gives improved estimates of the photoelectric cross sections and total mass attenuation coefficients at low energies. Other more recent evaluations (refs. D2 and H3) have revised the photoelectric coefficients, see Sec. 8e-3, herein, for discussion.

H1. Heitler, W.: "The Quantum Theory of Radiation," 3d ed., 430 pp., Oxford University Press, New York, 1954. Standard treatise on theory of interaction of photons with matter. No detailed experimental treatment.

H2. Hubbell, J. H.: Response of a Large Sodium-iodide Detector to High Energy X-rays, *Rev. Sci. Instr.* **29**, 65 (1958). A clearly explained example of the calculation of a 28-row by 28-column response matrix and inversion matrix for the case of a 5-in.-diameter by 4-in.-long NaI(Tl) crystal irradiated axially and centrally by well-collimated photons from 0.01 to 8 MeV.

H3. Hubbell, J. H., and M. J. Berger: Photon Attenuation and Energy Absorption Coefficients, Tabulations and Discussions, *Natl. Bur. Standards* (*U.S.*) *Rept.* 8681, 2d ed., 1966, 118 pp. Also to be published in "Engineering Compendium on Radiation Shielding," R. G. Jaeger, ed., IAEA, Vienna. An invaluable basic reference. The most recent among the series of critical evaluations of photon coefficients, intended to improve and extend the earlier numerical values given in refs. B5, D1, D2, G2, F2, I2, and W1. The tables cover 22 elements from H to U and 4 compounds and mixtures, mostly from 0.01 to 10 MeV, some to 100 MeV. Coefficients for total attenuation (μ_0/ρ), three types of absorption (μ_a/ρ), (μ_K/ρ), and (μ_{en}/ρ), and for the Compton, Rayleigh, photoelectric, and pair-production components are tabulated. These tables are based on the same smoothed-input data used for the tables in ref. E4, where a different selection of elements and many more mixtures are tabulated.

I1. International Commission on Radiological Units and Measurements (ICRU): Radiation Quantities and Units, report 10a, *Natl. Bur. Standards* (*U.S.*) *Handbook* **84** (1962). First promulgation of a revised set of definitions and units for use in radiological physics: kerma, fluence, exposure, mass energy-transfer coefficients, and others.

I2. International Commission on Radiological Units and Measurements (ICRU): Report of the ICRU for 1959, *Natl. Bur. Standards* (*U.S.*) *Handbook* **78** (1961). Definitions (some now superseded) of quantities and units for radiological physics, clinical, and biological factors; physical aspects of dosimetry; and measurement of radioactivity for radiological use.

J1. Johns, H. E., D. V. Cormack, S. A. Denesuk, and G. F. Whitmore: Initial Distribution of Compton Electrons, *Can. J. Phys.* **30**, 556 (1952). Tables for 10-keV to 30-MeV photons of the angular distribution of Compton scattered photons, the energy distribution and angular distribution of Compton recoil electrons.

M1. Miller, W. F., J. Reynolds, and W. J. Snow: Efficiencies and Photofractions for Sodium-iodide Crystals, *Rev. Sci. Instr.* **28**, 717 (1957); **30**, 141 (1959); and *Argonne Natl. Lab. Rept.* ANL-5902, 1958. Results of Monte Carlo calculations for NaI(Tl) crystals from 2 to 32 in. diameter and 1 to 8 in. length for 0.279- to 4.45-MeV photons from a parallel beam or from a point source or a disk source at 0, 6, 12, 18, or 30 in. distance along the crystal axis.

N1. Nelms, A. T.: Graphs of the Compton Energy-angle Relationship and the Klein-Nishina Formula from 10 keV to 500 MeV, *Natl. Bur. Standards Circ.* **542**, 1953, 89 pp. A succinct review of the Compton laws, the Klein-Nishina cross sections for unpolarized photons, and the incoherent scattering function, with 81 clear and accurate graphs.

P1. Price, B. T., C. C. Horton, and K. T. Spinney: "Radiation Shielding," Pergamon Press, London, 1957. Chapter 2 deals with broad-beam γ-ray attenuation and build-up factors, particularly with applications to the shielding of nuclear reactors.

W1. White, G. R.: X-ray Attenuation Coefficients from 10 keV to 100 MeV, *Natl. Bur. Standards Rept.* 1003, 1952. This mimeographed "first edition" of ref. G2 filled a great need and has been widely used. It contains on p. 17 a table of Compton "true absorption" coefficients $_e\sigma_a$ in which the low-energy values are incorrect but continue to be used by some workers (for example, ref. P1). Correct values of $_e\sigma_a$ and other Compton coefficients, over the same range of photon energies, are in ref. E2.

W2. Whyte, G. N.: "Principles of Radiation Dosimetry," John Wiley & Sons, Inc., New York, 1959, 124 pp. Physical principles and experimental methods for photon, electron, and neutron dosimetry.